Hypanus brevis: a newly resurrected Eastern South Pacific stingray lineage revealed by integrative taxonomy

Alan Marín[1*], Fabiola Zavalaga[2], Renato Gozzer-Wuest[3], Luis E. Santos-Rojas[1], Lorenzo E. Reyes-Flores[1], Ruben Alfaro[4], Philippe Béarez[5], Eliana Zelada-Mázmela[1]

[1] *Laboratorio de Genética, Fisiología y Reproducción, Facultad de Ciencias, Universidad Nacional del Santa, Chimbote, Perú*

[2] *Área Funcional de Investigaciones en Biodiversidad, Instituto del Mar del Perú - IMARPE, Callao, Perú*

[3] *Innovations for Ocean Action Foundation (I4OA), Lima, Peru*

[4] *Ecobiotech Lab S.A.C. Trujillo, Perú*

[5] *UMR 7209 BioArch, CNRS-MNHN, Muséum national d'Histoire naturelle, CP 56, 43 rue Buffon, 75005 Paris, France*

*Corresponding author

email amarin@uns.edu.pe

Abstract

Hypanus brevis (Garman, 1880) and *Hypanus dipterurus* (Jordan & Gilbert, 1880) are currently considered as a conspecific lineage of the "diamond stingray" from the Eastern Pacific. This taxonomic group has been the subject of nomenclatural disputes for about 145 years. To clarify the historical confusion surrounding this lineage, we employed an integrative taxonomic approach using specimens from the Eastern North and Eastern South Pacific (ENP and ESP). The genetic results, based on single and multilocus mitochondrial analyses, revealed a distinct evolutionary unit in the ESP. While morphological analyses detected subtle differences between ENP and ESP specimens, most characters exhibited significant overlap (e.g., disc shape, dentition patterns, body coloration), suggesting low evolutionary divergence. A calibrated molecular clock analysis estimated this divergence at approximately 3.09 Ma. In accordance with Garman's (1880) original description based on specimens from Paita (northern Peru), we formally resurrect *H. brevis* from synonymy with *H. dipterurus*. Our findings suggest an anti-tropical speciation pathway, with core populations of *H. brevis* and *H. dipterurus* restricted to the temperate waters of the ESP and ENP, respectively. Notably, a single, fixed COI haplotype was detected in all *H. brevis* specimens from the north-central Peruvian coast. This result may indicate a severe bottleneck event, raising concerns about the genetic health and long-term viability of this vulnerable species. Finally, we analyzed historical fishery data of *H. brevis* to infer its current population status, suggesting targeted conservation measures and precautionary management to prevent further loss of genetic diversity.

Keywords: Cryptic species, marine conservation, molecular phylogeny, Myliobatiformes, taxonomic resurrection

1. INTRODUCTION

Species of the genus *Hypanus* Rafinesque, 1818 (Myliobatiformes: Dasyatidae) are characterized by their wide pectoral fins that are fused to the head, a prominent row of thorns on nape and one or more thorns on shoulder in adults, a distinct but low ventral skin fold on tail (Last et al., 2016a). Most *Hypanus* species hold significant commercial value throughout their distribution range in the Atlantic and Pacific Oceans. They are either targeted by artisanal fisheries or frequently retained as valuable bycatch (Campos-León et al., 2025; Feitosa et al., 2021; Mejía-Falla et al., 2025). Due to their high market demand, unmanaged fishing practices, and their k-selected life history traits (Yamaguchi et al., 2021), half of the species in this genus are currently listed as threatened on The IUCN Red List (IUCN, 2025).

The genus *Hypanus* was considered a junior synonym of *Dasyatis*, until it was resurrected by Last et al. (2016b). It is now composed of eleven species (Fricke et al., 2025), including seven species from the Western Atlantic: *Hypanus americanus* (Hildebrand & Schroeder, 1928), *H. berthalutzae* Petean, Naylor & Lima, 2020, *H. geijskesi* (Boeseman, 1948), *H. guttatus* (Bloch & Schneider, 1801), *H. marianae* (Gomes, Rosa & Gadig, 2000), *H. sabinus* (Lesueur, 1824), and *H. say* (Lesueur, 1817); one species from the Eastern Atlantic: *Hypanus rudis* (Günther, 1870); and three species from the Eastern Pacific: *Hypanus dipterurus* (Jordan & Gilbert, 1880), *H. longus* (Garman, 1880), and *H. rubioi* Mejía-Falla, Navia, Cardeñosa & Tavera, 2025. However, a recent phylomitogenomic analysis suggested the existence of three additional evolutionary units within this genus (*H.* aff. *americanus*, *H.* aff. *guttatus*, and *H.* aff. *say*), warranting the need for a thorough taxonomic revision (Petean et al., 2024).

In the Eastern Pacific, the diamond stingray, *H. dipterurus*, is found from southern California (USA) to northern Chile (Almendras et al., 2025; Lamilla et al., 1995). This species is currently listed as Vulnerable on The IUCN Red List of Threatened Species, primarily due to

intense and largely unmanaged fisheries across most of its distribution range (Pollom et al., 2020). The diamond stingray is one of the most captured species by Mexican artisanal fisheries (Simental-Anguiano et al., 2022). In Colombia and Ecuador, its capture is limited to bycatch (Calle-Morán & Béarez, 2020; Puentes et al., 2022), while in Peru, artisanal fisheries target this species (Campos-León et al., 2025; González-Pestana et al., 2022). Despite its intense exploitation, high demand, and signals of population declines (Pollom et al., 2020), no formal management plans have been established in Peruvian stingray fisheries yet (González-Pestana et al., 2022). Furthermore, a long-standing taxonomic confusion with a junior synonym, *Dasyatis brevis* (Garman, 1880), may have skewed historical catch estimates. The diamond stingray has faced a long period of confused nomenclature history, due to two independent and nearly simultaneous descriptions published in 1880, that led to a confusing synonymy (Miller et al., 2014). The first description was published in May 1880 by Jordan and Gilbert, who named it *Dasybatis dipterurus* based on specimens collected from San Diego Bay in California (Jordan & Gilbert, 1880). Then, in October of the same year, Garman described *Trygon brevis*, based on two specimens from Paita, Peru (Garman, 1880). Garman (1913: 396) synonymized the two species (*D. dipterurus* and *T. brevis*) under the name *Dasybatus brevis*, considering wrongly that the date of publication of Jordan and Gilbert's work was 1881, thus giving priority to his own description from 1880. This inappropriate synonymization has led to long-standing ongoing confusion, dividing the opinion of modern researchers (Miller et al., 2014; Nelson et al., 2004; Nishida & Nakaya, 1990) until Eschmeyer (1998) recognized the nomenclatural priority of *D. dipterurus* Jordan & Gilbert, 1880 over *T. brevis* Garman, 1880. Ebert (2003), followed by Love et al. (2005) and Mundy (2005) then reclassified the latter as a junior synonym of *Dasyatis dipterura*, and finally Last et al. (2016b) reassigned the species to the genus *Hypanus* (currently *Hypanus*

dipterurus). Despite these taxonomic clarification efforts, the status of *H. dipterurus* and *D. brevis* remains controversial, even 145 years after their initial descriptions.

Inaccurate taxonomic revisions and hidden diversity can lead to a cascade of errors resulting in dire conservation consequences. This is particularly true for commercially exploited batoids, due to their high vulnerability to overfishing (Hosegood et al., 2020; White & Last, 2012). Treating multiple distinct species as a single group, or inversely, a single species managed as different units, can mask localized population declines and thus threaten the sustainability of these batoids (Chatzispyrou & Koutsikopoulos, 2023; Siskey et al., 2019). Furthermore, assessments of conservation status rely on the analysis of fisheries statistics from landing reports and geographical distributions based on taxonomic revisions (IUCN, 2024). The use of flawed catch statistics and imprecise distribution ranges resulting from taxonomic uncertainties can lead to inaccurate conservation status assessments (Marshall et al., 2009).

DNA sequence analysis represents a powerful tool for achieving taxonomic clarity, particularly in groups showing complex morphological identification, such as batoids, where traditional methods may fall short (Cunha et al., 2026; Marín, 2025; Sales et al., 2019; White et al., 2022). Genetic studies have played a crucial role in identifying hidden lineages within morphologically identical ray species, leading to significant formal taxonomic revisions (Last et al., 2016b; White et al., 2022). For example, a phylogenetic analysis of the southern stingray, *Hypanus americanus*, revealed that it was paraphyletic (Petean et al., 2020). This finding led to the discovery of a new species, the Lutz's stingray, *H. berthalutzae* by Petean et al. (2020). Additionally, genetic studies have led to the reinstatement of names that were previously treated as junior synonyms. These include the Indo-Pacific spotted eagle ray, *Aetobatus ocellatus* (Kuhl, 1823), which was previously considered a junior synonym of *A. narinari* (Euphrasen, 1790) (White et al., 2010); *Neotrygon trigonoides* (Castelnau, 1873),

135 previously synonymized with *N. kuhlii* (Müller & Henle 1841) (Borsa et al., 2013); and
136 *Zearaja brevicaudata* (Marini, 1933) (currently *Dipterurus brevicaudatus*), which was
137 confused with *Zearaja chilensis* (Guichenot, 1848) (currently *D. chilensis*) (Gabbanelli et al.,
138 2018), among others.
139 Most taxonomic and phylogenetic revisions including *H. dipterurus* samples have primarily
140 focused on populations from the Eastern North Pacific (hereafter referred to as ENP) (e.g.,
141 Last et al., 2016b; Naylor et al., 2012; Petean et al., 2020). On the other hand, the populations
142 of *H. dipterurus* from the Eastern South Pacific (hereafter referred to as ESP) have not yet
143 been assessed. Consequently, there is a significant knowledge gap regarding the connectivity
144 and gene flow among the populations from the northern and southern hemispheres.
145 Furthermore, a recent study suggested that *H. dipterurus* from the ESP may represent a
146 distinct evolutionary lineage (Petean et al., 2024). This study aims to evaluate the
147 evolutionary history and species boundaries of the Pacific diamond stingray, *H. dipterurus*.
148 First, we generated DNA sequences from *Hypanus* specimens collected in the ESP and
149 compared them with available conspecific sequences from the ENP populations. Then, we
150 provided a redescription of *H. dipterurus* from the ESP populations based on an integrative
151 taxonomic approach, which led to the formal resurrection of *H. brevis* (Garman, 1880).
152 Lastly, we evaluated historical and contemporary landing trends and discussed conservation
153 priorities and management strategies for sustainable *Hypanus* fisheries in the ESP.
154

155 ## 2. MATERIALS AND METHODS

156 All stingray samples used in this study were obtained from Peruvian artisanal fisheries,
157 landings, wholesale markets, local retail markets, and from activities conducted aboard
158 research vessels. Consequently, no animals were sacrificed specifically for the purposes of

this study and no special permissions were required as the target species are not under protection.

Specimens and tissue collection

The biological material used in this research was collected from January 2017 to January 2026. Four whole specimens of ESP *H. dipterurus* were collected and deposited in the Scientific Marine Collection of the Peruvian Marine Research Institute (IMARPE) under the catalog numbers IMARPE-020476 to IMARPE-020479. These include a juvenile caught as bycatch off Redondo Beach in Miraflores district, collected at the landing site "*Muelle de Pescadores*" in Chorrillos district (Peru). Three additional commercial specimens, caught at San José Beach in Lambayeque (Peru), were bought in a wholesale fish market located in Chiclayo city (Lambayeque, Peru) (see Table 1 and Figure 1). A small piece of tissue was excised from the oral epithelium of the buccal cavity of each sampled specimen using a sterile scalpel and preserved in ethanol 96 % for further DNA analysis. We also collected tissue samples from whole and incomplete specimens of ESP *H. dipterurus* and *H. longus* sourced from commercial fisheries, landings, aboard research vessels of IMARPE, and a wholesale fish market in the Lambayeque, Ica, and Tumbes regions (Peru). Additionally, tissue samples from *H. longus* were obtained from a local market in Huaquillas city (Ecuador). Small pieces of muscle from fillets, fins, and torsos were collected and preserved in commercial ethanol 96 % in 1.5 mL Eppendorf microtubes and stored at -15 °C until DNA extraction. Tissue samples obtained during IMARPE research activities were labeled with the prefix SV (without voucher specimens).

TABLE 1 List of samples analyzed in this study. GenBank and BOLD accessions are written between parentheses and brackets, respectively. ESP: Eastern South Pacific; ENP: Eastern North Pacific; Eastern Tropical Pacific: ETP.

Species name (Population)	Specimen Code	(GenBank)/[BOLD]		Collection date (MM/DD/YY)	Collection site	Geographic coordinates	Depth (m)	Country	Reference
		COI	16S rRNA						
Hypanus dipterurus (ESP)	ITPPL-073	[ITPPL073-14]	–	2014	Chorrillos (Lima)	–	–	PERU	Unpublished
	SF33	(MH194454)	(PZ027606)	01/24/2017	Tumbes (Tumbes)	–	–	PERU	Marín et al. (2018)
	SV-0063	(PZ027578)	(PZ027607)	06/08/2024	San José (Lambayeque)	6.9 S, 80.016667 W	–	PERU	This study
	SV-0146	(PZ027579)	(PZ027608)	06/03/2025	San José (Lambayeque)	6.767000 S, 80.547833 W	51	PERU	This study
	SV-0151	(PZ027580)	(PZ027609)	06/03/2025	San José (Lambayeque)	6.926667 S, 80.241333 W	53	PERU	This study
	SV-0153	(PZ027581)	(PZ027610)	06/03/2025	San José (Lambayeque)	6.871667 S, 80.393833 W	52	PERU	This study
	IMARPE-020476	(PZ027582)	(PZ027611)	10/25/2025	Miraflores (Lima)	–	10	PERU	This study
	IMARPE-0204777	(PZ027583)	(PZ027612)	11/11/2025	San José (Lambayeque)	–	–	PERU	This study
	IMARPE-0204778	(PZ027584)	(PZ027613)	11/11/2025	San José (Lambayeque)	–	–	PERU	This study
	IMARPE-0204779	(PZ027585)	(PZ027614)	11/11/2025	San José (Lambayeque)	–	–	PERU	This study
	HbLy-02	(PZ027586)	(PZ027615)	11/11/2025	San José (Lambayeque)	–	–	PERU	This study
	HbLy-05	(PZ027587)	(PZ027616)	11/11/2025	San José (Lambayeque)	–	–	PERU	This study
	HbLy-06	(PZ027588)	(PZ027617)	11/11/2025	San José (Lambayeque)	–	–	PERU	This study
	HbLy-07	(PZ027589)	(PZ027618)	11/11/2025	San José (Lambayeque)	–	–	PERU	This study
	HbLy-08	(PZ027590)	(PZ027619)	11/11/2025	San José (Lambayeque)	–	–	PERU	This study
	HbLy-09	(PZ027591)	(PZ027620)	11/28/2025	San José (Lambayeque)	–	–	PERU	This study
	HbLy-10	(PZ027592)	(PZ027621)	11/28/2025	San José (Lambayeque)	–	–	PERU	This study
	HbLa-01	(PZ027593)	(PZ027622)	11/28/2025	Puerto Chicama (La Libertad)	–	–	PERU	This study
	HbLa-02	(PZ027594)	(PZ027623)	11/28/2025	Puerto Chicama (La Libertad)	–	–	PERU	This study
	HbPi-01	(PZ027595)	(PZ027624)	01/––/2026	Pisco (Ica)	–	–	PERU	This study
	HbPi-02	(PZ027596)	(PZ027625)	01/––/2026	Pisco (Ica)	–	–	PERU	This study
	HbPi-03	(PZ027597)	(PZ027626)	01/––/2026	Pisco (Ica)	–	–	PERU	This study
	HbPi-04	(PZ027598)	(PZ027627)	01/––/2026	Pisco (Ica)	–	–	PERU	This study
	HbPi-05	(PZ027599)	(PZ027628)	01/––/2026	Pisco (Ica)	–	–	PERU	This study
	HbPi-06	(PZ027600)	(PZ027629)	01/––/2026	Pisco (Ica)	–	–	PERU	This study
	HbPi-07	(PZ027601)	(PZ027630)	01/––/2026	Pisco (Ica)	–	–	PERU	This study
	HbPi-08	(PZ027602)	(PZ027631)	01/––/2026	Pisco (Ica)	–	–	PERU	This study
Hypanus dipterurus (ENP)	MFC048	(GU440302)	–	09/27/2001	California	–	–	USA	Unpublished
	GN1598	Mitogenome (MZ381286)		06/16/2006	Gulf of California	25.916667 N, 110.416667 W	–	MEXICO	Petean et al. (2024)
	GN5379	Mitogenome (MZ381283)		10/24/2008	Baja California Sur	27.330833 N, 112.258333 W	–	MEXICO	Petean et al. (2024)
	GN5266	Mitogenome (MZ381284)		–	Baja California Sur	25.831111 N, 111.327222 W	–	MEXICO	Petean et al. (2024)
	GN5196	Mitogenome (MZ381285)		–	Baja California	28.985833 N, 113.548056 W	–	MEXICO	Petean et al. (2024)
	GN1598	[KERRI346-08]	–	2009	Gulf of California	23.8744 N, 101.554 W	–	MEXICO	Unpublished
	SEMAR-139	[SEMAR139-10]	–	05/19/2010	Manzanillo Bay	19.064 N, 104.305 W	–	MEXICO	Unpublished
	LPZSF31	(MT311551)	–	2018	–	–	–	MEXICO	Unpublished
Hypanus longus (ETP)	GN1599	Mitogenome (MT326628)		06/16/2006	Gulf of California	25.831111 N, 111.327222 W	–	MEXICO	Petean et al. (2020)
	GN5281	Mitogenome (MT326629)		10/24/2008	Gulf of California	23.045833 N, 109.6925 W	–	MEXICO	Petean et al. (2020)
	GN5282	Mitogenome (MT326630)		10/24/2008	Gulf of California	23.045833 N, 109.6925 W	–	MEXICO	Petean et al. (2020)
	GN5283	Mitogenome (MT326631)		10/24/2008	Gulf of California	23.045833 N, 109.6925 W	–	MEXICO	Petean et al. (2020)
	HlHu-01	(PZ027603)	(PZ027632)	06/02/2017	Huaquillas (El Oro)	–	–	ECUADOR	This study
	SV-0092	(PZ027604)	(PZ027633)	04/25/2024	Nuevo Paraíso (Tumbes)	3.762233 S, 80.821883 W	–	PERU	This study
	SV-0166	(PZ027605)	(PZ027634)	10/24/2024	Punta Pico (Tumbes)	3.727633 S, 80.805683 W	12.8	PERU	This study

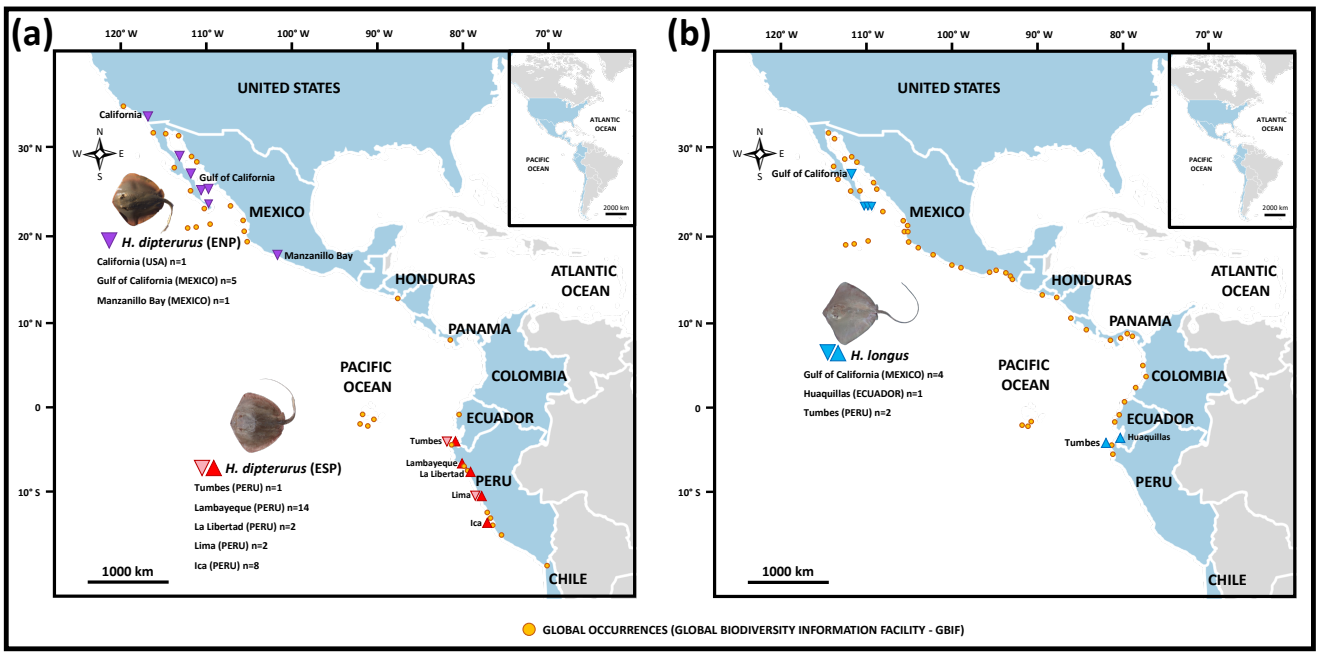

FIGURE 1 Sampling sites of *Hypanus* stingrays from the Eastern Pacific coast. Panel (a): Inverted purple triangles pinpoint sampling locations of *H. dipterurus* from the Eastern North Pacific (ENP) population with DNA sequences available in GenBank. Red triangles pinpoint sampling locations of *H. dipterurus* from the Eastern South Pacific (ESP) population collected in this study. Inverted pink triangles denote sampling sites of *H. dipterurus* samples whose DNA sequences were retrieved from the GenBank and BOLD databases. Panel (b): Inverted blue triangles indicate sampling locations of *H. longus* from the ENP population whose DNA sequences were retrieved from GenBank. Upright blue triangles indicate the sampling locations of *H. longus* from the ESP population collected in this study. Yellow circles represent global occurrences for *H. dipterurus* (a) and *H. longus* (b) as reported in the Global Biodiversity Information Facility (GBIF) database.

Molecular identification and data analyses

DNA isolation

Total genomic DNA was isolated using the cetyltrimethylammonium bromide (CTAB) protocol described by Zuccarello and Lokhorst (2005) with two modifications. In the organic extraction phase, the original chloroform:isoamyl alcohol (24:1) mixture was replaced with a phenol:chloroform:isoamyl alcohol in a final ratio of 25:24:1. During the subsequent DNA precipitation step, an additional 1/10 volume of sodium acetate (3 M, pH 5.2) was added to enhance precipitation efficiency. DNA quantification was estimated in an Epoch spectrophotometer (BioTek Instruments, Winooski, VT, USA). The genomic DNA was diluted to a final concentration of 50 ng/µL and used in PCR amplifications.

210 **PCR amplification**

211 A partial fragment (707 bp) of the mitochondrial COI gene was obtained using the universal
212 fish primer set FishF1 (5'-TCAACCAACCACAAAGACATTGGCAC-3') and FishR1 (5'-
213 TAGACTTCTGGGTGGCCAAAGAATCA-3') (Ward et al., 2005). For the amplification of
214 the mitochondrial 16S rRNA gene fragment (632 bp), we used the universal primers 16Sar-L
215 (5'-CGCCTGTTTATCAAAAACAT-3') and 16Sbr-H (5'-CCGGTCTGAACTCAGATCACG
216 T-3') (Palumbi et al., 1991). All PCR products were amplified in a total reaction volume of
217 10 µL with the following master mix composition: 0.1 µL of *Taq* polymerase 5 U/µL
218 (HiMedia, MBT060, Maharashtra, India), 0.9 µL of 10x PCR Buffer, 0.76 µL of $MgCl_2$ (25
219 mM), 0.5 µL of dNTPs (2.5 mM), 0.1 µL each primer (50 µM), 1 µL of genomic DNA (50
220 ng/µL), and 6.54 µL of ultrapure H_2O. Two different PCR amplification conditions were
221 used, depending on the DNA marker. For the COI marker, it consisted of an initial
222 denaturation for 5 min at 95 °C, followed for 35 cycles of denaturation step 30 s at 94 °C,
223 annealing for 40 s optimized from a range of 54-60 °C, and elongation for 60 s at 72 °C. A
224 final extension step was performed for 10 min at 72 °C. For the 16S rRNA, the initial
225 denaturation was 5 min at 95 °C, followed for 35 cycles of denaturation for 45 s at 94 °C,
226 annealing for 45 s at 58 °C, and elongation for 90 s at 72 °C. The final extension lasted 5 min
227 at 72 °C. Successful PCR amplifications were verified in a 1.5 % agarose gel electrophoresis.

228

229 **DNA sequencing**

230 Prior to DNA sequencing, PCR products were purified using FastAP Thermosensitive
231 Alkaline Phosphatase and Exonuclease I (Thermo Fisher Scientific, USA). Purified
232 amplicons were sequenced bi-directionally using the same primer sets and the BigDye
233 Terminator v3.1 Cycle Sequencing Kit (Applied Biosystems, Waltham, Massachusetts, USA)
234 on a ABI PRISM 3500 Genetic Analyzer (Applied Biosystems, Hitachi, Foster City, CA,

235 USA). All sequencing reactions were performed at the Laboratory of Genetics, Physiology,
236 and Reproduction of the National University of Santa. Electropherograms were visually
237 revised using MEGA 7 (Kumar et al., 2016), consensus sequences were obtained by aligning
238 forward and reverse complemented sequences, and primer positions were removed.
239

240 **Estimation of genetic diversity and population differentiation**

241 We used Arlequin v3.5 (Excoffier & Lischer, 2010) to quantify genetic variation within each
242 analyzed *H. dipterurus* population (ENP and ESP) and to estimate diversity metrics. These
243 include haplotype number, haplotype diversity "*Hd*", nucleotide diversity "π". The
244 relationships among haplotypes resulting from the COI and COI + 16S rRNA datasets were
245 assessed using Median-joining networks in HaplowebMaker tool (Spöri & Flot, 2020). To
246 assess deviations from selective neutrality and infer historical demographic events, we
247 calculated Fu's F_S and Tajima's D in both datasets (COI and COI + 16S rRNA) using
248 Arlequin. Statistical significance was evaluated with 10,000 coalescent simulations, with
249 threshold significance levels set at $P < 0.02$ (F_S) and $P < 0.05$ (D).
250 To quantify the degree of genetic divergence between the *H. dipterurus* samples collected
251 from ENP and ESP populations, we used the Analysis of Molecular Variance (AMOVA)
252 implemented in Arlequin. Pairwise fixation indices (Φ_{CT}, Φ_{SC}, and Φ_{ST}) were estimated using
253 the K2P distance model (Kimura, 1980) for the COI and concatenated COI + 16S rRNA
254 datasets. Accordingly, total variance was grouped into the following components: Φ_{CT}:
255 variation among groups, Φ_{SC}: variation among populations within groups, and Φ_{ST}: variation
256 among all populations. Two populations were defined: 1) the ENP population, comprising 8
257 DNA sequence samples sourced from GenBank, whose geographic origin indicated
258 California in the USA, and Gulf of California and Manzanillo Bay in Mexico; 2) the ESP
259 population, represented by 27 DNA sequences of which 25 sequences were determined in

260 this study (Ica region n = 8, Lambayeque region n = 14, La Libertad region n = 2, and Lima
261 region n = 1). Two additional Peruvian sequences were sourced from GenBank (Tumbes
262 region n = 1) and BOLD (Lima region n = 1) databases.
263

264 **Bayesian phylogenetic analysis**

265 The phylogenetic relationships among the DNA sequences of *Hypanus* species were inferred
266 using two independent Bayesian analyses based on single COI locus dataset and a
267 concatenated COI + 16S rRNA multilocus dataset. The partitioned Bayesian approach on the
268 multilocus dataset was conducted to enhance the phylogenetic signal of the 16S rRNA gene
269 and improve the reliability of species delimitation (Nylander et al., 2004). Although a
270 preliminary single-locus analysis of the 16S rRNA gene recovered ESP *H. dipterurus* and
271 ENP *H. dipterurus* as separate clades, the relatively low genetic distance (K2P: 1.7 %)
272 indicates a recent divergence between these two clades. Such shallow genetic divergences are
273 often associated with limited phylogenetic signal (Philippe et al., 2011). This may result in
274 weakly supported topology or overly confident statistical nodal support (Chen et al., 2017).
275 The single (COI) and multilocus (COI + 16S rRNA) datasets consisted of 55 and 50
276 sequences, respectively. These included 25 sequences for ESP *H. dipterurus* (Peru) and three
277 sequences for *H. longus* (Ecuador and Peru) determined in this work. They were analyzed
278 along with all available conspecific sequences from Mexico and the USA that were retrieved
279 from BOLD and GenBank databases. Additionally, four sequences of *H. say* (sister taxon of
280 *H. dipterurus*) and *H. americanus* (sister taxon of *H. longus*), and two sequences of *H.*
281 *sabinus* (sister taxon to all *Hypanus* species) (Mejía-Falla et al., 2025; Petean et al., 2024;
282 Rosenberger, 2001), were retrieved from the databases and included in the analyses. Two
283 bluespotted stingrays (*Neotrygon indica* Pavan-Kumar, Kumar, Pitale, Shen & Borsa, 2018
284 and *N. kuhlii*, subfamily Neotrygoninae) and the Daisy stingray (*Fontitrygon margarita*

285 (Günther, 1870), subfamily Urogymninae) were used as outgroups. DNA sequences from the
286 COI and 16S rRNA genes were aligned independently and trimmed using MEGA 7. Pairwise
287 genetic distances were calculated using the Kimura 2-parameter model (K2P, Kimura, 1980),
288 as implemented in MEGA 7. We assessed signals of nucleotide saturation in the protein-
289 coding COI dataset using DAMBE 7 (Xia, 2018). Next, the best-fit model of evolution for
290 each aligned matrix were assessed with jModelTest2 (Darriba et al., 2012) under the
291 corrected Bayesian Information Criterion (BICc). The best evolutionary model for the COI
292 and 16S rRNA gene datasets were HKY + G and HKY + I, respectively.
293 The Bayesian phylogenetic analyses were conducted in MrBayes 3.2.7 (Ronquist et al., 2012),
294 as implemented on the CIPRES Science Gateway 3.3 server (Miller et al., 2010). The
295 analyses were conducted with the data partitioned by gene and codon position. In both
296 datasets, the COI and the concatenated COI + 16S rRNA, the setup parameters consisted of
297 two independent runs of four Markov chains each, conducted for 10,000,000 generations.
298 Trees were sampled every 1,000 generations and the first 25 % of the sampled trees were
299 discarded as burn-in. Quality check of output files consisted on an Average Standard
300 Deviation of Split Frequencies (ASDSF) below 0.01 and Effective Sample Sizes (ESS) for all
301 parameters exceeding 200. The ESS were verified in Tracer v1.7.2 (Rambaut et al., 2018).
302 The consensus trees were visualized with FigTree version 1.4.4. (http://tree.bio.ed.ac.uk/soft
303 ware/figtree/).
304

305 **Calibrated molecular dating analysis**

306 To estimate the divergence times among target *Hypanus* species, we conducted a relaxed
307 molecular dating analysis based on the multilocus (COI + 16S rRNA) dataset. Since the two
308 previous phylogenetic analyses (single and multilocus) consistently recovered ESP *H.*
309 *dipterurus* and ENP *H. dipterurus* as distinct monophyletic clades, for the final molecular

dating we applied a more general model across the partitions: the GTR + I + G. To ensure taxonomic consistency with previous related studies, the following constraints were enforced *a priori*: root, crown *Hypanus*, ENP *H. dipterurus* monophyly, ESP *H. dipterurus* monophyly, ENP *H. dipterurus*/ESP *H. dipterurus* sister taxa, Panama Isthmus node 1 (*H. say*/*Hypanus* clade ancestor), Panama Isthmus node 2 (*H. longus/H. americanus*), and Dasyatinae node (Aschliman et al., 2012).

Node ages were calibrated using and "offsetlognormal" or "uniform" distribution based on established fossil or geological events. These include a) Root Dasyatidae: calibrated with and offsetlognormal(94.0, 100.0, 0.5) million years ago (Ma), to establish the minimum age of the Dasyatidae family based on *Dasyatis* fossil teeth record from the Cenomanian stage (Late Cretaceous) (Landemaine, 1991). b) The Dasyatinae node: calibrated via offsetlognormal(57.4, 64.9, 0.5) Ma, based on the *Dasyatis*/*Urogymnus* split age estimated by Aschliman et al. (2012) and applied following the updated classification of Last et al. (2016b). c) Crown *Hypanus*: calibrated with offsetlognormal(33.0, 40.0, 1.0) Ma, which corresponds to the divergence age of the *D. brevis* (currently *H. dipterurus*) during the Early Oligocene estimated by Aschliman et al. (2012), aligned with the taxonomic revision by Last et al. (2016b). d) Two transisthmian splits between *H. americanus*/*H. longus* and *H. say*/ENP *H. dipterurus*: each calibrated with offsetlognormal(3.1, 3.5, 0.5) Ma. We applied a lognormal(-5.2, 1.0) prior to the mean clock rate to model the typical slow mitochondrial mutation rate of 0.2-0.3 % per million years of chondrichthyan taxa (Martin et al., 1992).

The molecular clock analysis was conducted using the same Bayesian settings as in the phylogenetic inference described in the previous subsection, with the exception that the MCMC run was increased to 50,000,000 generations to reach stationary.

Morphometric and meristic analysis

Morphometric and meristic analyses were conducted on four complete, fresh specimens of *Hypanus* (Table 1), following primarily Petean et al. (2020), with additional measurements taken from Jordan and Gilbert (1880). All body measurements were taken in a straight line using a caliper with a precision of 0.1 mm; measurements exceeding 170 mm were taken using dividers and read with a steel ruler with a precision of 1 mm. After measurements, specimens were fixed in 10 % formalin, rinsed, preserved in 70 % ethanol, and deposited in the IMARPE Scientific Collection under the catalog numbers IMARPE-020476, IMARPE-020477, IMARPE-020478, and IMARPE-020479. Comparative morphometric data were obtained from the original descriptions of *Trygon brevis* by Garman (1880), considering the two syntypes under the collection number MCZ Ichthyology S-422, one female and one male from Paita, Peru; and from Lamilla et al. (1995). We compared with morphometric data of two syntypes of *Dasybatis dipterurus* from Jordan and Gilbert (1880) description; and with those given by Beebe and Tee-Van (1941) and Nishida and Nakaya (1990). Measurements are expressed in millimeters (mm) and in percentages (%) of the disc width (% DW). In some cases, measurements originally expressed in inches were converted to millimeters. When necessary, measurements were also standardized from proportions of total length (TL) or disc length (DL) to ensure comparability. Taxonomic validity and nomenclature follow Fricke et al. (2025), while collection codes are based on Sabaj (2020). All specimens from the IMARPE fish collection were also used for species identification through genetic analyses.

Fishery data analysis

A database of chondrichthyan landings from 1996 to 2024, geolocated by fishing zones, was provided by the IMARPE, in response to a request for access to public information under Peruvian transparency provisions. In total, the database comprised 182,282 landing records,

classified by geolocation (latitude and longitude), fishing gear, common and scientific names, year, and landed volume. Records of batoid species, particularly those classified as *Dasyatis brevis* and the generic scientific designation *Hypanus* sp., were filtered to describe small-scale fishing activity targeting species under analysis. Consequently, both labels were extracted for descriptive purposes. Additionally, fishing areas of the small-scale fisheries were classified into four zones by latitude: Tropical North, North, Center, and South, based on IMARPE's classification available in the Peruvian Atlas of Small-Scale Fisheries (Marín-Soto et al., 2017). Additionally, the distance to the coast of the reported catches was estimated using the Fenix R Studio package (Marín-Abanto, 2018). The data were used to estimate trends in landings and to show the marine areas within the Peruvian Sea with the highest occurrence of this species' fishing activity. Furthermore, to discover its economic value, annual average off-vessel prices and total monetary landing values were estimated using open-access data collected and stored by IMARPE (2025). Nearly 2,108 records of nominal off-vessel prices for the research target species from 2009 to 2024 were obtained. The nominal off-vessel prices were converted from Peruvian soles (PEN) to US dollars (USD) using monthly PEN/USD exchange rates published by the Peruvian Central Bank (BCRP, 2025a). Additionally, nominal prices were converted to real prices by deflating them using the consumer price index (CPI), published monthly by the BCRP from January 1991 onwards, with December 2021 as the baseline (i.e., IPC = 100) (BCRP, 2025b).

3. RESULTS

DNA sequencing

We successfully obtained genomic DNA, PCR products, and DNA sequences from all specimens collected from the ESP populations. These include 25 sequences for *H. dipterurus* and three sequences for *H. longus*. After the removal of the primer sequences, the DNA

385 sequences for the COI and 16S rRNA markers were 655 bp and 590 bp in length, respectively.
386 All DNA sequences generated in this research were assigned the following GenBank
387 accessions: from PZ027578 to PZ027605 for the COI gene and from PZ027606 to PZ027634
388 for the 16S rRNA gene.
389
390 **Genetic diversity indexes and neutrality tests**
391 *Hd* for both the single locus and multilocus datasets, was high (0.8571 and 0.8333,
392 respectively) in *H. dipterurus* samples from the ENP population. Conversely, the *Hd* in the
393 ESP population was zero for the COI dataset due to the fixation of a single haplotype, while
394 the combined COI + 16S rRNA dataset yielded an *Hd* of 0.1477. π followed a similar pattern,
395 being higher in the ENP (COI: 0.003461, COI + 16S rRNA: 0.000906), and notably lower in
396 the ESP population (COI: 0.0, COI + 16S rRNA: 0.000134) (see Table 2). Neutrality test for
397 the ENP yielded negative values for both the Fu's F_S and Tajima's *D*. Although these values
398 were not significant in all cases, their negative trend deviates from expectations of a neutral
399 population model and may reflect a recent population expansion. Neutrality test from the ESP
400 could not be calculated for the COI gene due to the lack of polymorphism. However, the
401 combined COI + 16S rRNA dataset, which contained two haplotypes, resulted in a non-
402 significant Fu's F_S (-0.3167, P = 0.1648) and a Tajima's *D* of 0.000 (P = 1.000). While these
403 values suggest no significant departures from mutation-drift equilibrium, this is likely an
404 artifact of the extremely low genetic diversity (e.g., one COI haplotype for 27 specimens),
405 which limits the statistical power to detect demographic shifts. This lack of variation is
406 consisted with a founder effect associated with a recent speciation event or a severe historical
407 bottleneck.
408
409

410 **TABLE 2** Summary results of genetic diversity indices and Fu's *F s*and Tajima's *D* neutrality tests for single
411 locus dataset (COI) and multilocus dataset (COI + 16S rRNA) of *H. dipterurus*. ENP: Eastern North Pacific
412 population, ESP: Eastern South Pacific population. Genetic diversity includes: number of haplotypes (h),
413 haplotype diversity (*Hd*), and nucleotide diversity (π). Sample size: n. N.A.: Not Applicable.
414

Population	Marker	n	h	*Hd* ± S.E.	π	Fu's F_S*	Tajima's *D***
ENP (Mexico-USA)	COI	8	5	0.8571 ± 0.1083	0.003461± 0.002537	-1.40322 (P = 0.08330)	-1.06428 (P = 0.16190)
	COI + 16S rRNA	4	3	0.8333 ± 0.2224	0.000906 ± 0.000897	-0.88730 (P = 0.08860)	-0.70990 (P = 0.28510)
ESP (Peru)	COI	27	1	0.0000 ± 0.0000	0.0000 ± 0.0000	0.0000 (P = N.A.)	0.0000 (P = 1.0000)
	COI + 16S rRNA	26	2	0.1477 ± 0.0888	0.000134 ± 0.000219	-0.31678 (P = 0.16480)	0.0000 (P = 1.0000)

415 * P < 0.02 significant.
416 ** P < 0.05 significant
417

418 ## Haplotype network analysis

419 The median-joining haplotype network analyses for *H. dipterurus* samples from the ENP and
420 ESP populations are presented in Figure 2. Our haplotype network findings from the single
421 locus and concatenated multilocus datasets revealed a clear genetic divergence between both
422 the ENP and ESP populations. In the COI haplotype network (top panel in Figure 2a), five
423 haplotypes were observed in samples from the ENP population (Mexico n = 7; USA n = 1),
424 while a single private haplotype represented the ESP population (Peru, n = 27). The branch
425 connecting the unique haplotype of the ESP haplogroup (H1b) to the closest haplotype from
426 the ENP (H1d, Gulf of California) displayed a genetic distance of 18 stepwise mutations. The
427 largest genetic distance (23 nucleotides) between both haplogroups was detected between
428 haplotypes H1b (Peru) and H5d (Gulf of California). The haplotype network obtained using
429 the concatenated COI + 16S rRNA dataset (bottom panel in Figure 2a) resulted in a dominant
430 haplotype H1b for the ESP population (Peru, n = 24), while a single satellite haplotype H2b
431 was found in only two individuals. These two ESP haplotypes were separated by a single
432 mutational step, represented by a deletion that was observed in the 16S rRNA gene from two
433 specimens collected in Pisco (Ica region, GenBank accessions PZ027624 and PZ027626).
434 The ESP haplogroup was distanced by 30 mutational steps to closest haplotype H1d in the

435 ENP haplogroup, which comprised a total of three haplotypes from four specimens collected
436 in Mexico. This substantial genetic distance and lack of shared haplotypes between the two
437 haplogroups (ESP and ENP) strongly suggest that they represent isolated evolutionary units.
438 On the other hand, the haplotype networks of both datasets (COI and COI + 16S rRNA) from
439 *H. longus* suggest the existence of a single lineage across the Eastern Pacific (top and bottom
440 panels in Figure 2b, respectively). A unique dominant haplotype was detected in each
441 population (ENP: Mexico, ESP: Ecuador and Peru), with three and five stepwise mutations
442 between each haplotype in the single locus and multilocus datasets, respectively.
443
444

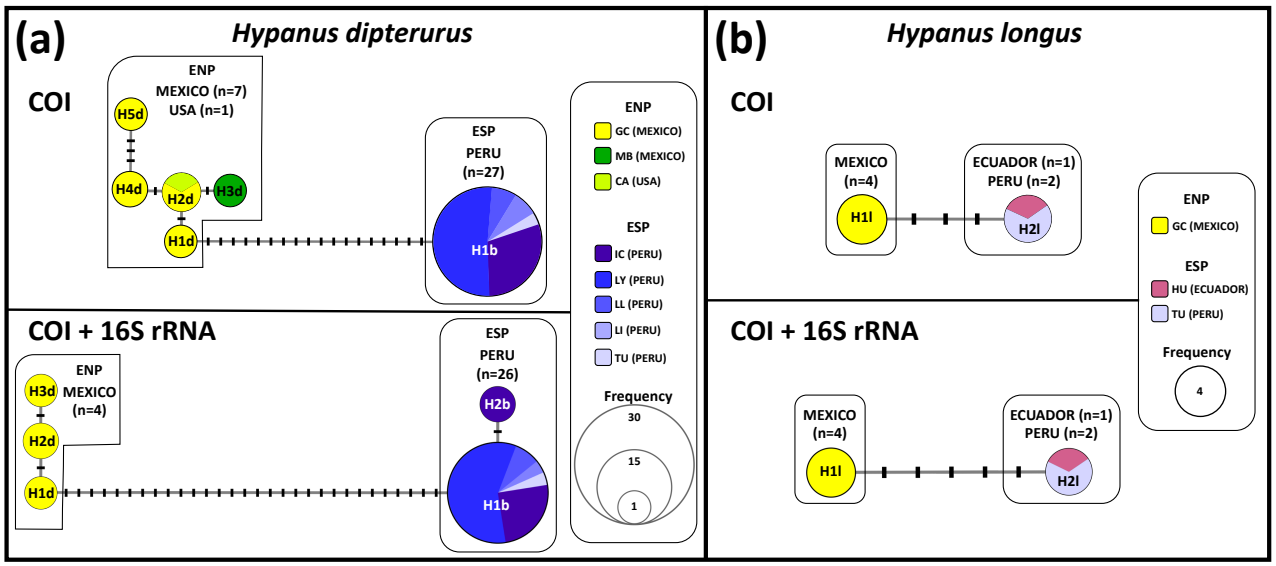

445 **FIGURE 2** Median joining network analysis illustrating the genetic relationships and geographical distribution
446 of two *Hypanus* lineages using DNA sequences from samples collected in the Eastern North Pacific (ENP) and
447 Eastern South Pacific (ESP) populations. Panel (a): Haplotype network of *H. dipterurus* based on COI
448 sequences (above) and concatenated sequences from COI + 16S rRNA (below). Panel (b): Haplotype network
449 of *H. longus* based on COI sequences (above) and concatenated sequences from COI + 16S rRNA (below).
450 Circles (nodes) represent unique haplotypes, where its size is proportional to the frequency of that haplotype in
451 the sampled population. Perpendicular bars across the lines connecting haplotypes represent single mutational
452 steps. Colors denote the geographic origin of the samples. In the ENP population: yellow color for the Gulf of
453 California (GC) and green for Manzanillo Bay (MB), both in Mexico. Electric lime color for California (CA) in
454 the USA. In the ESP population: raspberry pink for Huaquillas (HU) in Ecuador. Purple color for the Ica region
455 (IC), electric blue color for the Lambayeque region (LY), neon blue for the La Libertad region (LL), pale blue
456 for the Lima region (LI), lavender blue for the Tumbes region (TU), all located in Peru.
457
458

459 **Analysis of Molecular Variance (AMOVA)**

460 The AMOVA results (Table 3) revealed significant differences in the molecular data for both
461 datasets. For the single locus (COI) dataset, a vast majority of the variation (97.54 %)
462 occurred between both *H. dipterurus* groups (ENP vs ESP), while only a minor variation was
463 observed within populations (2.49 %). Similarly, in the combined multilocus (COI + 16S
464 rRNA) dataset, a higher level of variation (99.25 %) was detected between groups. These
465 results strongly suggest a genetic isolation based on geographic location of the ENP and ESP
466 groups. Fixation indices further supported the genetic divergence between ENP and ESP
467 populations. The Φ_{CT} values, which measure differentiation among groups, were notably high
468 at 0.97 (P = 0.02) for COI and 0.99 (P = 0.16) for the combined data. Additionally,
469 consistently high Φ_{ST} values (0.98 and 0.99, P = 0.00) confirm complete genetic isolation and
470 lack of gene flow between the analyzed groups.

471

472 **TABLE 3** Results of the Analysis of Molecular Variance (AMOVA) and fixation indices (Φ_{CT}, Φ_{SC}, and Φ_{ST})
473 based on single locus (COI) and multilocus (COI + 16S rRNA) datasets from DNA sequences of *Hypanus*
474 *dipterurus*. Two groups were compared: ENP (Eastern North Pacific: Mexico and USA) population group and
475 ESP (Eastern South Pacific: Peru) population group.
476

Dataset	Source of Variation	d.f.	Variance Components	% of Variation	Fixation Indices	P-value
COI (Single)	Among groups	1	9.46466 Va	97.54	Φ_{CT} = 0.97536	0.02053
	Among populations within groups	6	-0.00257 Vb	-0.03	Φ_{SC} = -0.01077	0.65396
	Within populations	20	0.24167 Vc	2.49	Φ_{ST} = 0.97510	0.00000
COI + 16S rRNA (Combined)	Among groups	1	15.22730 Va	99.25	Φ_{CT} = 0.99249	0.16618
	Among populations within groups	4	-0.00976 Vb	-0.06	Φ_{SC} = -0.08466	0.36364
	Within populations	24	0.12500 Vc	0.81	Φ_{ST} = 0.99185	0.00000

477 Fixation indices significant at P < 0.05

478

479

480

481 **Bayesian phylogenetic analysis**

482 The Bayesian phylogenetic analyses of both, the single (Figure 3a) and multilocus (Figure
483 3b) datasets, further supports the conclusions drawn from the haplotype network and
484 AMOVA findings. In both phylogenetic trees, DNA sequences from ENP and ESP *H.*
485 *dipterurus* populations were recovered in two discrete monophyletic clades at the top of the
486 trees with strong nodal support. The sister relationship between both *H. dipterurus*
487 populations exhibited a COI genetic distance ranging from 3.6 % (± 0.008) to 4.6 % (±
488 0.010), with an average value of 4 % (± 0.009) (Table S1). This genetic distance range is
489 substantially higher than the interspecific genetic threshold reported in congeneric species
490 (Petean et al., 2024). Our phylogenetic findings, combined with the haplotype network and
491 AMOVA results, provide robust evidence that *H. dipterurus* populations from ENP and ESP
492 constitute distinct evolutionary lineages.

493 Conversely, the results of the Bayesian phylogenetic analyses support the existence of a
494 single Pacific lineage for *H. longus*. In both Bayesian phylogenetic trees, corresponding to
495 the COI and concatenated COI + 16S rRNA dataset, all *H. longus* samples were recovered
496 within a single monophyletic group with high statistical support (Figure 3). They displayed
497 low COI intraspecific genetic distance, ranging from 0 to 0.6 % (± 0.003), which is lower
498 than the standard interspecific DNA barcoding gap reported in species from this genus
499 (Petean et al., 2024).

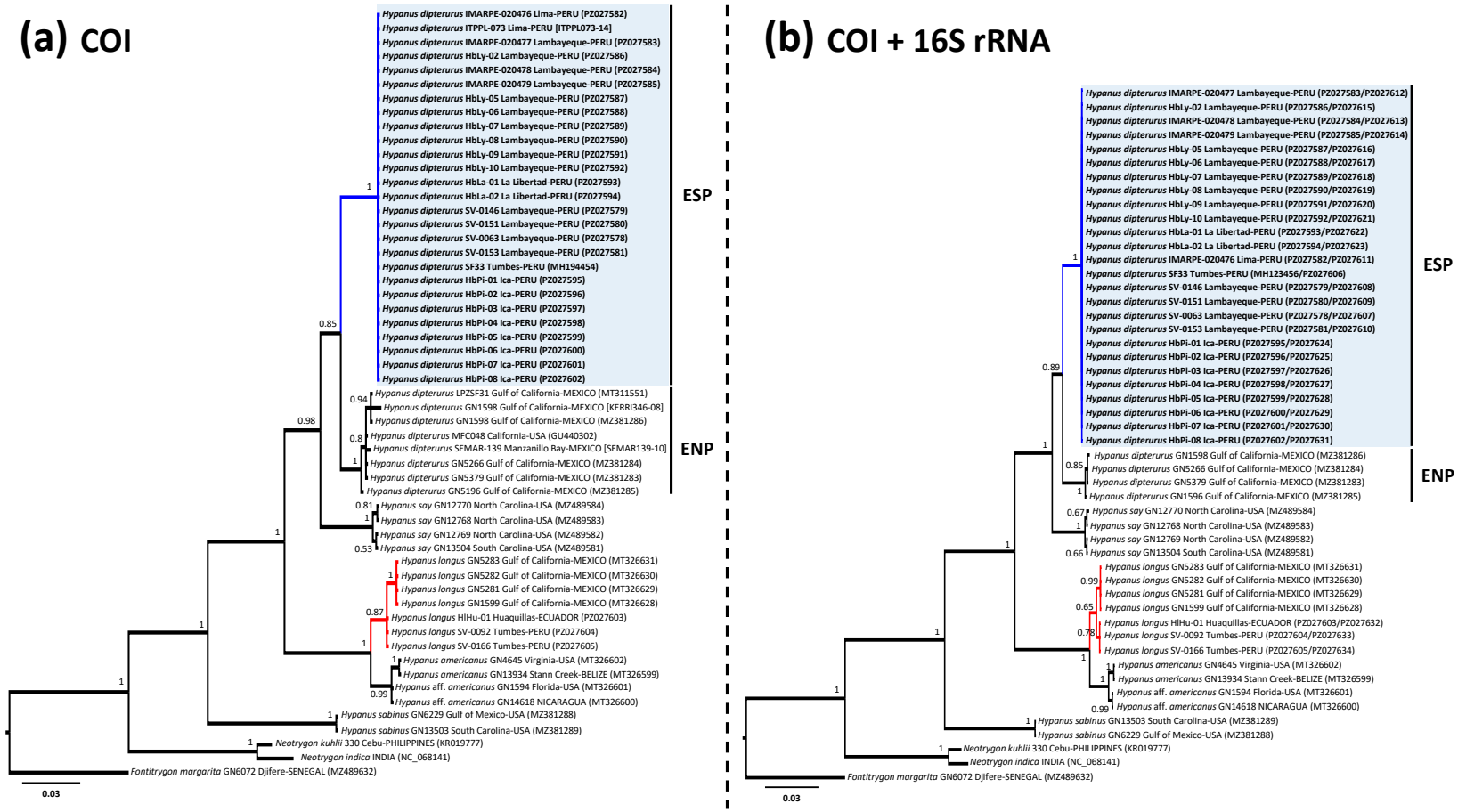

FIGURE 3 Bayesian phylogenetic trees showing the evolutionary relationships among stingrays in the genus *Hypanus*. Panel (a) shows the phylogenetic tree constructed using a single locus COI marker (substitution model: HKY + G) and the tree from Panel (b) utilized the concatenated information from the COI + 16S rRNA genes (substitution model: HKY + I). Each label shows the species scientific name, voucher name, geographical origin (when available), and GenBank (between parentheses) or BOLD (between brackets) accessions numbers. The numbers next to each node indicate the Bayesian Posterior Probability. To distinguish *H. dipterurus* from the Eastern North Pacific (ENP) and Eastern South Pacific (ESP) populations, the clade grouping all samples from the ESP population is highlighted in blue color and shaded in sky blue color. The *H. longus* clade is highlighted in red color. *Hypanus sabinus*, the sister taxa to all *Hypanus* group, was used as an internal outgroup. Two bluespotted stingrays (*Neotrygon kuhlii* and *N. indica*) and the Daisy stingray (*Fontitrygon margarita*) were used as external outgroups.

Calibrated molecular clock analysis

The calibrated Bayesian molecular clock analysis dated the most recent common ancestor (MRCA) of the Dasyatidae lineage (subfamilies Dasyatinae, Neotrygoninae, and Urogymninae) at approximately 120.89 Ma, during the Early Cretaceous (Figure 4). The major Dasyatinae clade divergence occurred around the Cretaceous-Paleogene (K-Pg) boundary, at approximately 64.88 Ma. The crown *Hypanus* radiation started about 39.98 Ma, during the Late Eocene. The divergence of the common ancestor of the Atlantic *H. americanus* and *H. say* occurred approximately 24.62 Ma during the Early Miocene. The most recent *Hypanus* divergences occurred during the Late Pliocene. These include two transisthmian divergence events that resulted in the formation of the geminate species *H. say* (Atlantic) and *H. dipterurus* (Pacific) (3.42 Ma), and *H. americanus* (Atlantic) and *H. longus* (Pacific) (3.43 Ma). Finally, the most recent speciation event occurred within the diamond stingray *H. dipterurus*, when the ESP *H. dipterurus* lineage branched off from its geminate from the ENP, at approximately 3.09 Ma (Figure 4).

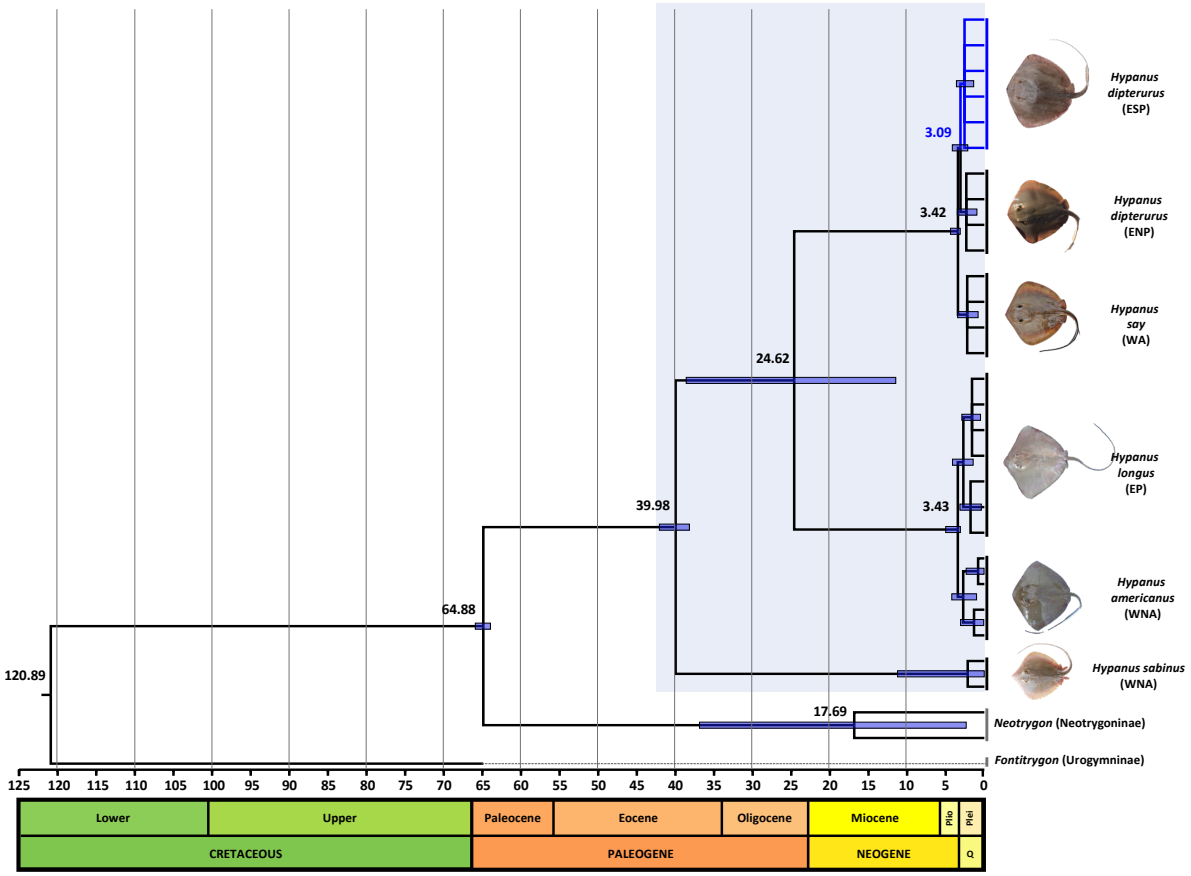

FIGURE 4 Relaxed Bayesian time-calibrated phylogeny illustrating the evolutionary relationships and estimated divergence of six target *Hypanus* species: *H. americanus*, *H. dipterurus*, *H. longus*, *H. sabinus*, and *H. say*. The crown *Hypanus* ingroup (subfamily Dasyatinae) is shaded in light blue. Outgroups include two *Neotrygon* species: *N. kuhlii* and *N. indica* (subfamily Neotrygoninae) and *Fontitrygon margarita* (subfamily Urogymninae). The ESP *H. dipterurus* clade, which is identified as a distinct linage that was split from the ENP *H. dipterurus*, is highlighted in blue. Node ages represent the estimate divergence times in million years. Blue horizontal bars indicate the 95 % highest posterior density (HPD) intervals. The scale bar shows the geological time scale in millions of years, with periods ranging from the Cretaceous to the Quaternary (Q). Plei: Pleistocene Epoch, Plio: Pliocene Epoch. Species distributions: EP (Eastern Pacific), ESP (Eastern South Pacific), ENP (Eastern North Pacific), WA (Western Atlantic), WNA (Western North Atlantic). Photograph credits: image of ESP *H. dipterurus* by F. Zavalaga; image of *H. longus* was taken by L. Bancayán; images of *H. americanus*, *H. sabinus*, and *H. say* were kindly provided by R. Robertson (Robertson & Van Tassell, 2023); image of ENP *H. dipterurus* was retrieved from the iNaturalist database (2026).

Based on the findings of this research, which strongly support that *H. dipterurus* populations from the ENP and ESP represent isolated evolutionary units, we propose that the ESP lineage be formally recognized as *H. brevis*. This taxonomic assignment follows Garman's (1880) original description based on specimens from Paita, northern Peru. The revalidation of *H. brevis* increases the number of recognized species to 12 and brings the total number of distinct *Hypanus* evolutionary units to 15 (Table 4), including the three molecular evolutionary units (*H.* aff. *americanus, H.* aff. *guttatus, and H.* aff. *say*) identified by Petean et al. (2024).

TABLE 4 Current accepted species and latest taxonomic changes in members of the genus *Hypanus*. Distribution: EP (Eastern Pacific), ESP (Eastern South Pacific), ENP (Eastern North Pacific), ETP (Eastern Tropical Pacific), WA (Western Atlantic), EA (Eastern Atlantic), ECA (Eastern Central Atlantic), WCA (Western Central Atlantic), WNA (Western North Atlantic), WSA (Western South Atlantic), Gulf of Mexico (GM), NB (Northern Brazil), SB (Southern Brazil), and CS (Caribbean Sea).

Taxonomy	Common name	Description Year	Distribution	Original name	Latest taxonomic change	Reference	IUCN status
Genus							
Hypanus Rafinesque, 1818	Stingrays	1818	EP, WA, EA	*Hypanus* Rafinesque, 1818	Resurrected from synonymy with *Dasyatis*	Last et al. (2016b)	2 as CR (18.1 %) 1 as EN (9.1 %) 3 as VU (27.3 %) 3 as NT (27.3 %) 1 as LC (9.1 %) 1 as NE (9.1 %)
Validated species by the present work							
Hypanus brevis (Garman, 1880)	Peruvian diamond stingray	1880	ESP	*Trygon brevis* Garman, 1880	Resurrected from synonymy with *H. dipterurus*	This study	VU (needs reassessment)

Validated species in the literature							
Hypanus guttatus (Bloch & Schneider, 1801)	Longnose stingray	1801	WCA to SB	*Raja guttata* Bloch & Schneider, 1801	Moved from the genus *Dasyatis* (*D. guttata*)	Last et al. (2016b)	NT
Hypanus say (Lesueur, 1817)	Bluntnose stingray	1817	WA	*Raja say* Lesueur, 1817	Moved from the genus *Dasyatis* (*D. say*)	Last et al. (2016b)	NT
Hypanus rudis (Günther, 1870)	Smalltooth stingray	1870	ECA	*Trygon rudis* Günther, 1870	Moved from the genus *Dasyatis* (*D. rudis*)	Last et al. (2016b)	CR
Hypanus dipterurus (Jordan & Gilbert, 1880)	Diamond stingray	1880	ENP	*Dasybatis dipterura* Jordan & Gilbert, 1880	Moved from the genus *Dasyatis* (*D. dipterura*)	Last et al. (2016b)	VU (needs reassessment)
Hypanus longus (Garman, 1880)	Longtail stingray	1880	ETP	*Trygon longa* Garman, 1880	Moved from the genus *Dasyatis* (*D. longa*)	Last et al. (2016b)	VU
Hypanus sabinus (Lesueur, 1824)	Atlantic stingray	1824	WNA	*Trygon sabina* Lesueur, 1824	Moved from the genus *Dasyatis* (*D. sabina*)	Last et al. (2016b)	LC
Hypanus americanus (Hildebrand & Schroeder, 1928)	Southern stingray	1928	WNA, WCA and CS	*Dasyatis americana* Hildebrand & Schroeder, 1928	Moved from the genus *Dasyatis* (*D. americana*)	Last et al. (2016b)	NT
Hypanus geijskesi (Boeseman, 1948)	Wingfin stingray	1948	WCA, NB	*Dasyatis geijskesi* Boeseman, 1948	Moved from the genus *Fontitrygon*	Petean et al. (2024)	CR
Hypanus marianae (Gomes, Rosa & Gadig, 2000)	Brazilian large-eyed stingray	2000	WSA (Brazil)	*Dasyatis marianae* Gomes, Rosa & Gadig, 2000	Moved from the genus *Dasyatis* (*D. marianae*)	Last et al. (2016b)	EN
Hypanus berthalutzae Petean, Naylor & Lima, 2020	Lutz's stingray	2020	WSA (Brazil)	*Hypanus berthalutzae* Petean, Naylor & Lima, 2020	New discovery. It was split from *H. americanus*	Petean et al. (2020)	VU
Hypanus rubioi Mejía-Falla, Navia, Cardeñosa & Tavera, 2025	Pointed-nose Pacific stingray	2025	ETP	*Hypanus rubioi* Mejía-Falla, Navia, Cardeñosa & Tavera, 2025	New discovery	Mejía-Falla et al. (2025)	NE
Molecular evolutionary units (aff.)							
Hypanus aff. *americanus*	–	–	WNA, WCA, CS	–	–	Petean et al. (2024)	–
Hypanus aff. *guttatus*	–	–	WCA	–	–	Petean et al. (2024)	–
Hypanus aff. *say*	–	–	GM	–	–	Petean et al. (2024)	–

Resurrection of *Hypanus brevis* (Garman, 1880)

Trygon brevis Garman, 1880: 171. Description.

Dasibatis brevis Garman (1883: 70).

Dasybatus brevis. In part Garman (1913: 396). Specimens of Paita, Peru, pl. 32, figs. 5-6.

Dasyatis brevis Chirichigno (1974: 75, figs. 67-68); Lamilla et al. (1995: 23-27); Chirichigno & Vélez (1998: 65, figs. 11-12); Chirichigno & Cornejo (2001: 67).

Hypanus dipterurus. Almendras et al. (2025), specimens of Peru and Chile.

Syntypes collected in Paita, Peru (MCZ Ichthyology S-422; Georeferenced as 5° 9' S, 81° 8' W or -5.1583333°, -81.141666°; collection date May 5, 1872; collector Hassler expedition). Held at the Museum of Comparative Zoology, Harvard University.

https://mczbase.mcz.harvard.edu/guid/MCZ:Ich:S-422

Although Garman (1880) did not mention collection numbers, it is assumed that there are at least two syntypes. He indicated Paita (Piura, Peru) as the locality of origin for at least one of the specimens (female) mentioned in his description and confirmed the provenance of the two measured specimens (male and female) as Peru (Garman, 1883). He made no reference to type material from California.

Diagnosis

A large-sized diamond-shaped species of *Hypanus* (attaining at least 900 mm DW) with the following combination of characters: body slightly wider than long; snout pointed but not elongated, rostral length 18.5–20.7 % DW; anterolateral margins of disc nearly straight, forming an angle of 124–130°; disc length 82.5–87.0 % DW; internostril width 8.5–9.7 % DW; oral papillae five, arranged in a transverse row on the floor of the mouth, with three well-developed medial papillae and one minute lateral papilla on each side; tail whiplike, less than 1.25 times disc width (1.4–1.5 times disc length), bearing a long, slender caudal spine and a short ventral caudal fin fold (25.7–34.6 % DW); dorsal disc generally smooth in

607 juveniles, adults with scattered scapular denticles and enlarged denticles anterior to the
608 caudal spine; coloration brown to olive-brown dorsally, lacking spots.
609

610 **Description**

611 Disc wider than long, disc length equivalent to 82.5–87 % of disc width (DW). Anterolateral
612 margins of disc nearly straight, posterior margins convex. Snout pointed but not protruding,
613 forming an angle of 124–130°. Upper and lower jaws with small, blunt teeth. Oral papillae
614 five, arranged in a single transverse row on the floor of the mouth; three medial papillae large
615 and well developed, and one-minute lateral papilla on each side, widely separated from the
616 medial group. Pelvic fins broad, with truncate margins, slightly rounded apices, and rounded
617 angles.
618 Tail moderately long, with a length equivalent to 119–123 % of disc width; broad and
619 slightly depressed at the base, progressively tapering toward the caudal spine. Dorsal and
620 ventral folds present on tail; dorsal fold low and short, ventral fold higher and longer than
621 dorsal, representing 25.73–34.63 % of disc width. Ventral fold originates at level of caudal
622 spine basis, dorsal fold at level of caudal spine tip. Both folds terminate at approximately the
623 same level along the tail, from where the tail begins to compress, subsequently narrowing
624 into a filament.
625 Dorsal surface of disc smooth. The largest specimen (IMARPE-20479), a female of 540 mm
626 DW, exhibits an irregular row of scattered denticles extending from the nuchal region to the
627 origin of the caudal spine, as well as a short row on each shoulder, with up to five denticles
628 per side. Juvenile specimens lack denticles. Additionally, a large incomplete specimen
629 collected at ~6° S (SV-0063) showed more than 14 prominent, broad-based denticles on the
630 tail prior to the caudal spine (see Figure 5).

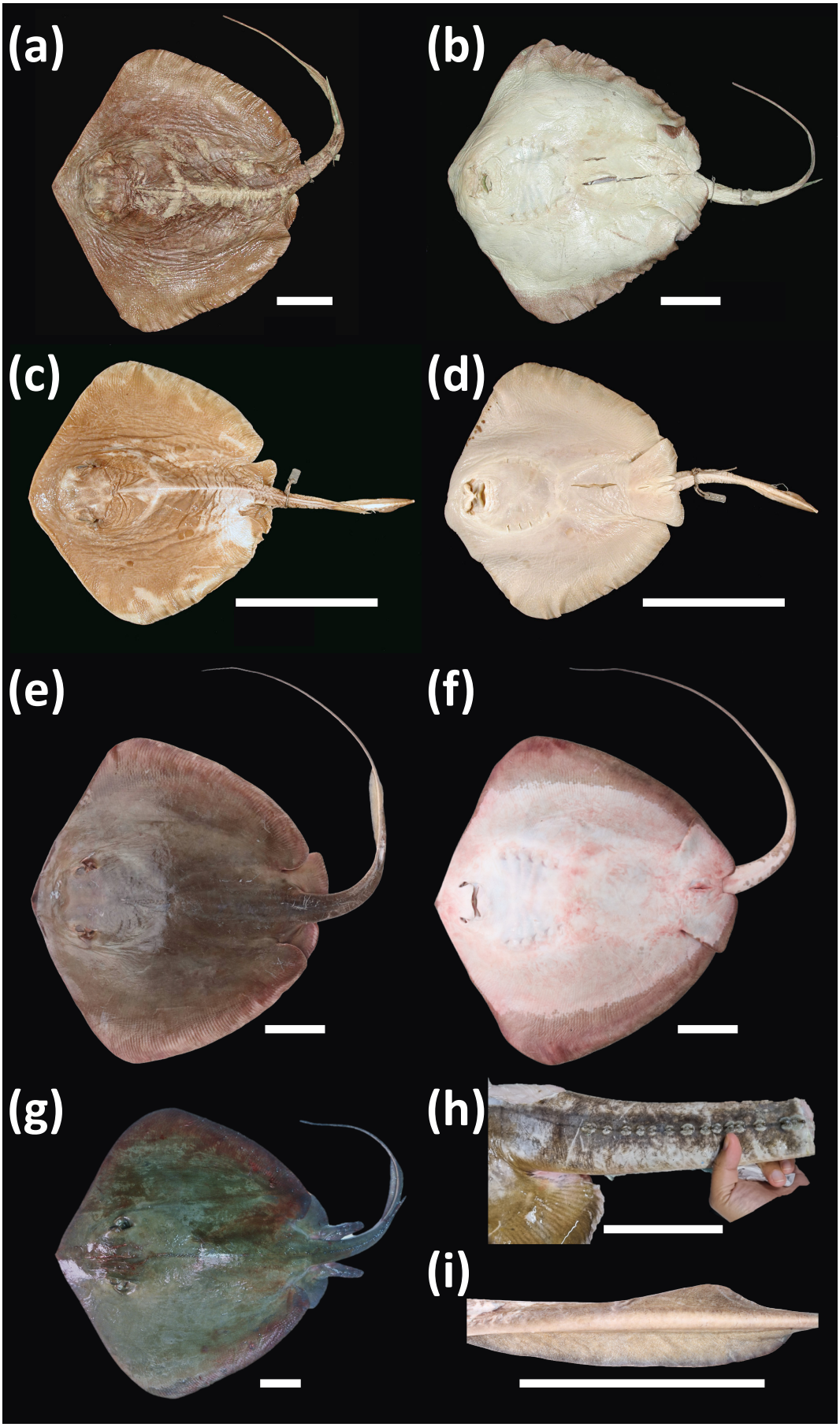
(a)
(b)
(c)
(d)
(e)
(f)
(g)
(h)
(i)

FIGURE 5 *Hypanus brevis* (Garman, 1880) from Peruvian waters. (a)–(d) Dorsal and ventral views of the syntypes of *Trygon brevis* Garman, 1880, female and male collected in Paita, MCZ S-422. (e)–(f) Dorsal and ventral views of female specimen IMARPE-20479 (present study). (g) Dorsal view of a male specimen collected in Chorrillos, MNHN-ICOS-02627 (TL = 1265 mm, DW = 690 mm). (h) Tail of specimen SV-0063 showing prominent, broad-based denticles (ca 900 mm DW). (i) Dorsal and ventral tail folds of specimen IMARPE-20479. Photographic credits: (a), (b), (c) and (d) Museum of Comparative Zoology, Harvard University; (e), (f), and (i) A. Moreno; (g) P. Béarez; and (h) F. Zavalaga. Scale bar: 10 cm.

Comparison

Hypanus brevis is distinguished from its Eastern Pacific congeners *H. longus* and *H. rubioi* by having a very short tail, measuring 1.4–1.5 times disc length vs 2.4 times in *H. longus* and 2.4–3.1 times in *H. rubioi*. Tail length in *H. brevis* is similar to that of *H. dipterurus*, which ranges from 1.1 to 1.4 times disc length (Jordan & Gilbert 1880; Beebe & Tee-Van 1941; Mejía-Falla et al., 2025). *Hypanus brevis* shares with *H. longus* a disc that is wider than long, with disc length values ranging from 82.5 to 87.0 % DW in *H. brevis* and 81.6 to 86.8 % DW in *H. longus*. In contrast, *H. brevis* differs from *H. dipterurus*, in which disc length represents a higher proportion of disc width, ranging from 88.9 to 94.9 % DW. In *H. rubioi*, disc length is slightly greater, with values ranging from 89.6 to 98.2 % DW, resulting in a disc that is nearly as long as wide. *Hypanus brevis* does not have a pointed nor elongated rostrum, with rostral length ranging from 18.5 to 20.7 % of disc width (DW), compared to 29.5-32.1 % DW in *H. rubioi*. In this respect, *H. brevis* shares a similar rostral length with *H. longus* (16.4-19.5 % DW) and *H. dipterurus* (15.9–21.8 % DW). However, the rostral angle is markedly wide in *H. brevis* (124–130°) and *H. dipterurus*, slightly less wide in *H. longus*, whereas it is acute in *H. rubioi*. *H. brevis* shares with *H. dipterurus* a small ventral caudal fin fold, 25.7-34.6 % DW and 28.4-33.3 % DW, respectively. In contrast, *H. longus* and *H. rubioi* have a longer ventral caudal fin fold, measuring 45–52.4 % DW and 38–60.8 % DW, respectively. The internostril width is smaller in *H. brevis* (8.5–9.7 % DW) compared to *H. dipterurus* (13.6-18.6 % DW). In contrast, values for *H. longus* (9.4–10.4 % DW) and *H. rubioi* (9.1–10.7 % DW) are similar to, though slightly higher than, those observed in *H. brevis*.

Color in life

Dorsal surface uniformly brown, dark brown, or olive-brown, becoming slightly reddish near the margins (see Figure 6); ventral surface white, with the posterior margins of the pectoral and pelvic fins brown. Juveniles exhibit a slightly more violaceous coloration on the dorsal surface.

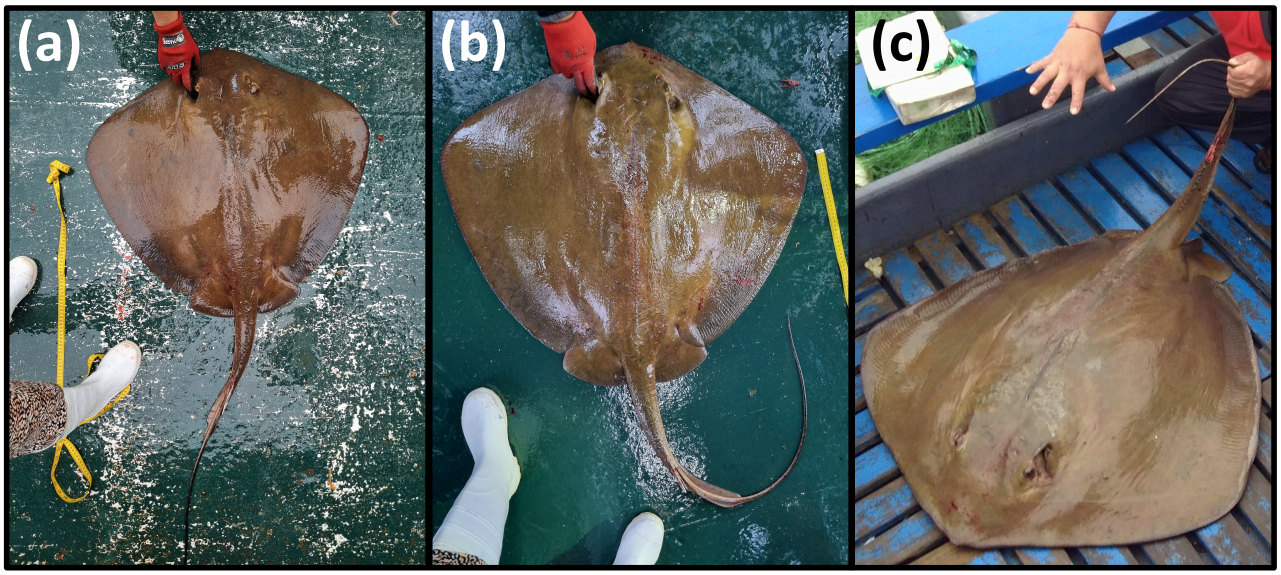

FIGURE 6 *Hypanus brevis* (Garman, 1880) Pictures illustrating the coloration observed in recently caught/live specimens. Panels (a) and (b): female specimens (SV-0146 and SV-0151, respectively) caught in San José (Lambayeque region, Peru); (c): specimen collected in Pisco (Ica region, Peru). Photographic credits: (a) and (b) F. Zavalaga; (c) J. Quiñones (used with written permission).

TABLE 5 Morphometric and meristic characteristics of *Hypanus brevis* (Garman, 1880) based on specimens collected in the southern Pacific Ocean off Peru, expressed in millimeters and as percentages of disc width (%DW). Data for the syntypes are taken and compared from Garman (1880), specimens MCZ S-422 from Paita, Peru. Additional comparisons are made with data from Garman (1913); Lamilla et al. (1995); and from the syntypes of *H. dipterurus* Jordan and Gilbert (1880), from Beebe and Tee-Van (1941), and Nishida and Nakaya (1990). *Data corrected from the original publication. (–) (?) Data not reported.

Species	**This study, *Hypanus brevis* n=4**								***H. brevis*** (Garman, 1880) (Syntypes)				***H. brevis*** (Lamilla et al., 1995)				***H. dipterurus*** (Jordan & Gilbert, 1880)				***H. dipterurus*** (Beebe & Tee-Van, 1941)			***H. dipterurus*** (Nishida & Nakaya, 1990)	
Museum catalogue N°	**IMARPE-20479**		**IMARPE-20478**		**IMARPE-20477**		**IMARPE-20476**		**MCZ S-422**		**MCZ S-422**		**IZUA-PM 1433**		**w/n**		**No.1**		**No.2**		**24,943**		**24,995**	**LACM 31759-16**	
Measurements	**mm**	**%DW**	**mm**	**%DW**	**mm**	**%DW**	**mm**	**%DW**	**mm**	**%DW**	**mm**	**%DW**	**mm**	**%DW**	**mm**	**%DW**	**mm**	**%DW**	**mm**	**%DW**	**mm**	**%DW**	**mm**	**mm**	**%DW**
Total length TL	1140	211.11	614	206.04	658	204.98	483	200.41	-	-	-	-	510	205.60	-	-	-	-	-	-	1257	175.44	702	466.9	207.4
Angle of the rostrum (°) AR	130	-	128	-	129	-	124	-	-	-	-	-	125	-	-	-	-	-	-	-	-	-	-	-	-
Disc width DW	540	100.00	298	100.00	321	100.00	241	100.00	457.2	100.00	233.7	100.00	248	100.00	600	100.00	231.1	100.00	237.5	100	716.49	100.00	-	225.1	100.0
Disc length DL	470	87.04	253	84.90	265	82.55	206	85.48	431.8	94.44	205.8	88.06	218	87.90	505	84.20	222.2	94.87	215.9	90.91	672.50	93.86	331.34	200.1	88.9
Mouth to tail MtT	367	67.96	255	85.57	222	69.16	167	69.29	-	-	-	-	-	-	-	-	-	-	-	-	-	-	-	-	-
Pre-caudal length PCL	462	85.55	253	84.90	267	83.18	205	85.06	-	-	-	-	-	-	-	-	-	-	-	-	-	-	-	-	-
Snout to cloaca length StC	420	77.77	220	73.83	240	74.77	187	77.59	-	-	-	-	194	78.20	435	72.50	155.57	66.40	151.1	63.63	-	-	-	176.5	78.4
Cloaca to caudal tip length CtCT	732	135.55	387	129.87	430	133.96	288	119.50	-	-	-	-	-	-	-	-	-	-	-	-	-	-	-	-	-
Pre-spine length PSL	605	112.04	320	107.38	347	108.10	265	109.96	-	-	-	-	-	-	-	-	-	-	-	-	-	-	-	253.7	112.7
Caudal length CL	663	122.77	360	120.81	398	123.99	289	119.92	584.2	127.77	304.8	130.42	315	127.00	-	-	311.15	132.82	315	132.6	734.09	102.46	370.66	-	-
Caudal width at spine CSW	16	2.96	8	2.68	7	2.18	6	2.49	-	-	-	-	-	-	-	-	-	-	-	-	-	-	-	-	-
Tail origin to spine origin length TSL	160	29.63	85	28.52	93	28.97	71	29.46	-	-	-	-	-	-	-	-	-	-	-	-	-	-	-	-	-
Caudal width at P2 end CW	39	7.22	18.5	6.21	17	5.30	14	5.81	-	-	-	-	-	-	-	-	-	-	-	-	-	-	-	-	-
Caudal height at pelvic fin end CH	24	4.44	12	4.03	12	3.74	9.5	3.94	-	-	-	-	5	2.00	13	2.20	-	-	-	-	-	-	-	-	-
Caudal length postventral fold CLPF	347	64.26	202	67.79	224	69.78	149	61.83	-	-	-	-	-	-	-	-	-	-	-	-	-	-	-	-	-
Dorsal caudal fold height DFH	10	1.85	3.5	1.17	5	1.56	3	1.24	-	-	-	-	1.1	1.90	8.8	1.50	3.9	1.69	4.1	1.73	-	-	-	-	-
Dorsal caudal fold length DFL	78	14.44	36.5	12.25	34	10.59	38	15.77	-	-	-	-	31.4	12.70	76.5	12.80	30	12.81	33.5	14.09	-	-	-	-	-
Ventral caudal fold height VFH	16	2.96	4	1.34	8	2.49	3.5	1.45	-	-	-	-	4.6	1.90	10.6	1.80	5	2.11	4.9	2.06	-	-	-	-	-
Ventral caudal fold length VFL	187	34.63	77	25.84	88	27.41	62	25.73	-	-	-	-	66.7	26.90	160	26.70	66.7	28.46	78.8	33.18	-	-	-	74.9	33.3
Pelvic fin posterior margin P2PM	107	19.81	40	13.42	63	19.63	32.5	13.49	-	-	-	-	-	-	-	-	-	-	-	-	-	-	-	-	-
Pelvic fin length P2L	104	19.26	52	17.45	57	17.76	42	17.43	-	-	-	-	40	16.10	103	17.20	-	-	-	-	-	-	-	-	-
Pelvic fin anterior margin P2AM	93	17.22	48	16.11	54	16.82	42	17.43	-	-	-	-	-	-	-	-	-	-	-	-	-	-	-	-	-
Pelvic fin width P2W	112	20.74	38	12.75	55	17.13	33	13.69	-	-	-	-	-	-	-	-	-	-	-	-	-	-	-	-	-
Clasper internal length CIL	-	-	8	2.68	-	-	9	3.73	-	-	-	-	-	-	-	-	-	-	-	-	-	-	-	-	-
Clasper external length CEL	-	-	9	3.02	-	-	9	3.73	-	-	-	-	16.7	6.70	-	-	-	-	-	-	-	-	-	-	-
Head length HDL	190	35.19	122	40.94	130	40.50	103	42.74	-	-	-	-	105*	42.30*	-	-	71.12	30.36	72.32	30.45	-	-	-	94.9	42.2
Preorbital length POBL	100	18.52	57	19.13	60	18.69	50	20.75	-	-	-	-	45	18.10	124	20.70	46.7	19.92	38.9	16.36	155.87	21.75	77.22	35.8	15.9
Pre-oral length POL	87	16.11	47	15.77	51	15.89	41	17.01	-	-	-	-	40	16.10	85.8	14.30	-	-	-	-	123.19	17.19	54.76	-	-
Pre-nasal length PNL	68	12.59	37	12.42	40	12.46	33	13.69	-	-	-	-	31.7	12.80	69	11.50	-	-	-	-	91.76	12.81	44.93	-	-
Internostril width INW	46	8.52	27	9.06	29	9.03	23.5	9.75	-	-	-	-	22	8.90	50.6	8.40	34.4	14.7	32.4	13.63	133.24	18.60	-	-	-
Nasal curtain length NCL	28	5.19	14	4.70	14	4.36	13	5.39	-	-	-	-	-	-	-	-	-	-	-	-	-	-	-	-	-
Nasal curtain width NCW	56	10.37	28	9.40	33	10.28	25	10.37	-	-	-	-	-	-	-	-	-	-	-	-	-	-	-	-	-
Mouth width MW	46	8.52	27	9.06	27	8.41	21	8.71	-	-	-	-	22.9	9.20	52.8	8.80	24.4	10.44	23.7	10	54.05	7.54	35.1	-	-
Mouth length to widest part of disc MWD	300	55.56	160	53.69	174	54.21	130	53.94	-	-	-	-	-	-	-	-	-	-	-	-	-	-	-	-	-
Distance from mouth to base of tail DMtT	400	74.07	205	68.79	225	70.09	165	68.46	-	-	-	-	-	-	-	-	-	-	-	-	-	-	-	-	-
Eye length EYL	23	4.26	12	4.03	13	4.05	10	4.15	-	-	-	-	10.9	4.40	17.5	2.92	-	-	-	-	-	-	-	15.1	6.7
Eye width EW	10	1.85	4	1.34	5.5	1.71	4	1.66	-	-	-	-	-	-	-	-	-	-	-	-	-	-	-	-	-
Interorbital length IOL	80	14.81	43	14.43	42	13.08	36	14.94	-	-	-	-	34	13.70	122	20.30	28.9	12.33	24.8	10.45	138.27	19.30	71.60	22.1	9.8
Interspiracle length ISL	91	16.85	49	16.44	57	17.76	43	17.84	-	-	-	-	48	19.40	110	18.30	-	-	-	-	-	-	-	-	-
Spiracle length SPL	41	7.59	24	8.05	24	7.48	20	8.30	-	-	-	-	18	7.30	22.5	3.80	-	-	-	-	-	-	-	-	-
Spiracle width SW	22	4.07	9	3.02	11	3.43	10	4.15	-	-	-	-	-	-	-	-	-	-	-	-	-	-	-	-	-
Width of branchial area (in front)	155	28.70	82	27.52	92	28.66	68	28.22	-	-	-	-	-	-	-	-	71.1	30.36	66.93	28.18	-	-	-	-	-
First gill slit width 1GW	20	3.70	9	3.02	11	3.43	8	3.32	-	-	-	-	7.5	3.00	21.6	3.60	-	-	-	-	-	-	-	-	-
Third gill slit width 3GW	22	4.07	10	3.36	13	4.05	9	3.73	-	-	-	-	9	3.60	25	4.20	-	-	-	-	-	-	-	-	-
Fifth gill slit width 5GW	16	2.96	9	3.02	9	2.80	7	2.90	-	-	-	-	6.5	2.60	19.9	3.30	-	-	-	-	-	-	-	-	-
Distance between first gill slits DB1GS	121	22.41	68	22.82	71	22.12	56	23.24	-	-	-	-	52.1	21.00	130	21.70	-	-	-	-	167.18	23.33	77.22	-	-
Distance between third gill slits DB3GS	108	20.00	60	20.13	62	19.31	47	19.50	-	-	-	-	-	-	-	-	-	-	-	-	-	-	-	-	-
Distance between fifth gill slits DB5GS	83	15.37	45	15.10	49	15.26	39	16.18	-	-	-	-	35	14.10	88.7	14.80	-	-	-	-	100.56	14.03	49.14	-	-
Distance between the first and fifth gill slits	87	16.11	46	15.44	49	15.26	37	15.35	-	-	-	-	-	-	-	-	43.34	18.5	38.86	16.36	-	-	-	-	-
Spine length SL	69	12.78	43	14.43	37	11.53	34	14.11	-	-	-	-	31.5	12.70	92.6	15.40	-	-	72.3	30.46	-	-	-	-	-
Distance from disk to dorsal fold	245	45.37	112	37.58	105	32.71	83	34.44	-	-	-	-	-	-	-	-	100	42.69	114.4	48.18	-	-	-	-	-
Distance from root of tail to ventral fold	138	25.56	70	23.49	75	23.36	62	25.73	-	-	-	-	-	-	-	-	84.4	36.05	81	34.09	-	-	-	-	-
Distance of spine from disk	135	25.00	67	22.48	82	25.55	59	24.48	-	-	-	-	-	-	-	-	77.8	33.21	70.17	29.55	-	-	-	-	-
Counts																									
Cross-series of teeth in the upper jaw	>10	-	>11	-	>12	-	>10	-	-	-	-	-	-	-	-	-	8	-	-	-	20	-	-	-	-
Cross-series of teeth in the lower jaw	20	-	16	-	17	-	>9	-	-	-	-	-	-	-	-	-	10	-	-	-	26	-	-	-	-
Papillae on floor of mouth	5	-	5	-	5	-	5	-	-	-	-	-	-	-	-	-	-	-	-	-	-	-	-	5	-
Sex	female		male		female		male		female		male		male		female		female		female		male		female	male	
Maturity	adult		juvenile		juvenile		juvenile		?		young		?		?		?		?		?		?	?	

Size

The largest known specimen of *H. brevis* is an incomplete mature individual of approximately 900 mm DW (SV-0063, present study), collected off Peru at ~6° S (Figure 5h). A male specimen 690 mm DW collected in Chorrillos, Lima, Peru, on 25 March 1999 (MNHN-ICOS-02627; Figure 5g) weighed 13800 g. In the present study, the specimens examined measured between 241 and 540 mm DW.

Distribution

Hypanus brevis and *H. dipterurus* have long been considered synonyms and widely distributed along the coastline of the ETP. However, recent evidence suggests that *H. brevis* is restricted to the southeastern Pacific (ESP). In South America, *H. dipterurus* has been reported in commercial fisheries off Ecuador (Calle-Morán & Béarez, 2020; Martínez-Ortiz & García-Domínguez, 2013) and Colombia (Mejía-Falla & Navia, 2019). These records may correspond to the northernmost occurrence of *H. brevis*; however, further genetic analyses are required to determine whether the diamond stingrays captured in these countries belong to *H. brevis* or *H. dipterurus*. To date, *H. brevis* has been genetically confirmed only from specimens collected in Peru. Southward, several studies have reported the presence of *H. brevis* south to Antofagasta, northern Chile (Almendras et al., 2025; Lamilla et al., 1995), which likely represents the southernmost limit of its distribution.

Common name

To differentiate *H. brevis* from its sister species, *H. dipterurus* (commonly known as the Diamond stingray), we propose the common name "Peruvian diamond stingray". This name is fitting because the original description is based on specimens collected from northern Peru.

As for the Spanish common name, the vernacular term "*batea*" is widely used in Peru as the commercial name for this particular species, and we suggest keeping it unchanged.

Fishery

Over 29 years, a total of 135 thousand tons of chondrichthyans were recorded in the IMARPE landing database. These figures account for 19 % of the batoid group, with less than 1 % potentially attributable to *H. brevis* (top panel of Figure 7). Notably, 98 % of these volumes were originally labeled by IMARPE as *Dasyatis brevis*, while the remaining were identified as *Hypanus* sp. Between 2015 and 2024, IMARPE recorded an annual catch of approximately 46.2 tons of *H. brevis* (*sd* of 12.3 tons), corresponding to an annual economic value of approximately 62,000 USD (*sd* of ± 16,000; see Figure S1). The majority of the landings were reported from northern regions of the country (44 %; averaging 20.4 ± 6.6 tons per year) and from the southern regions (37 %; averaging 16.8 ± 9.8 tons per year; bottom panel of Figure 7). During this period, 78 % of landings originated from gillnets, with the remaining percentage from unspecified fishing gear types other than gillnets (e.g., beach seines and purse seines as reported by González-Pestana et al., 2022).

The fishery for *H. brevis* is primarily coastal, with 32 % of reported catches occurring during 2015-2024 within the first nautical mile (nm) off the Peruvian coastline and an additional 44 % between 1-5 nm. The remaining catches, reported far from the 5 nm, are likely still within the continental shelf, as most of these catches occur around the *Lobos de Afuera* Islands (Figure 8).

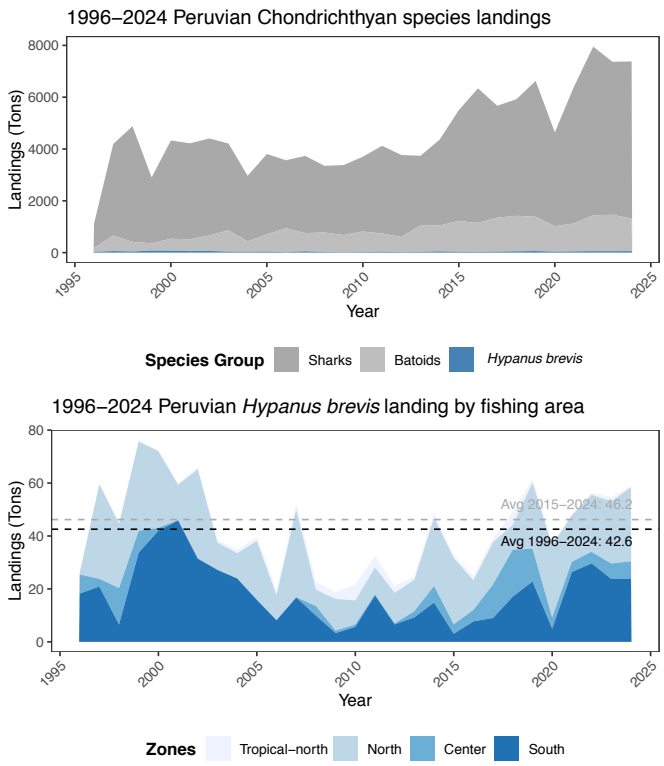

FIGURE 7 Peruvian Chondrichthyan species documented in the IMARPE landing data from 1996 to 2024 (top panel) and landings potentially attributable to *Hypanus brevis* within the same period (bottom panel).

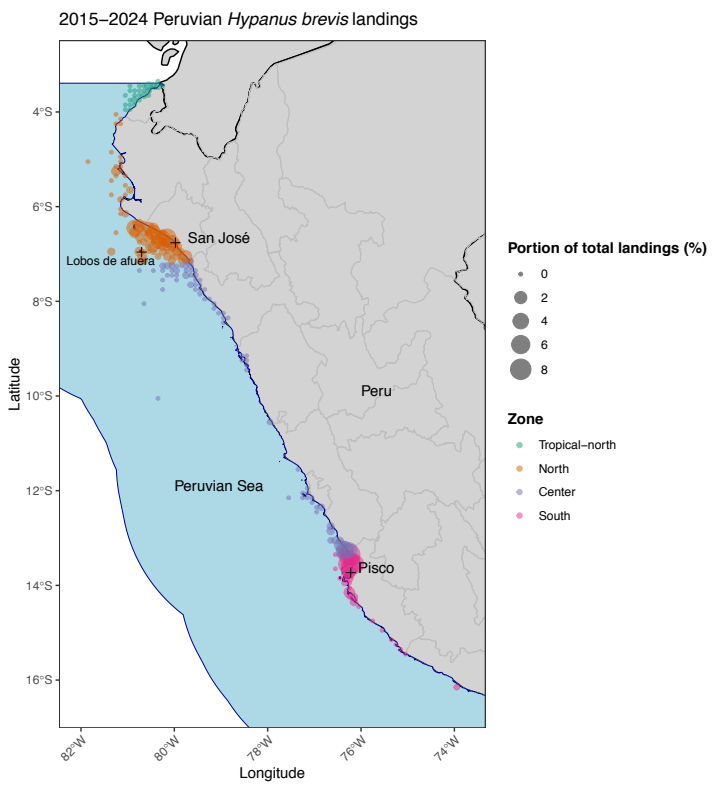

FIGURE 8 The occurrence of landings of *Hypanus brevis* in the Peruvian Sea from 2015 to 2024, classified within a 0.1° latitude by 0.1° longitude grid.

829 **4. DISCUSSION**

830 Allopatric speciation is a major evolutionary model that has shaped the population history of
831 most aquatic species, including elasmobranchs (Ball et al., 2016; Gayford & Jambura, 2025).
832 This evolutionary mechanism has been a primary driver of species richness in batoids (Staggi
833 et al., 2025), which comprises more than a half of all elasmobranch diversity (Ebert et al.,
834 2017). The speciose nature of this elasmobranch group, coupled with its highly conserved
835 morphology (dorsoventrally flattened bodies and countershaded coloration), have led to a
836 long history of inaccurate taxonomic descriptions (Chatzispyrou & Koutsikopoulos, 2025;
837 Last et al., 2016b).

838 This issue is particularly evident in the genus *Hypanus*, whose taxonomic composition has
839 been subjected to major controversy, with significant revisions performed since the last
840 decade (Last et al., 2016b). Most of these taxonomic revisions (see Table 4) were
841 accomplished by means of integrative taxonomic approaches, including DNA information
842 from complete mitogenomes or partial gene sequences (Last et al., 2016b; Mejía-Falla, et al.,
843 2025; Petean et al., 2020; Petean et al., 2024). Nevertheless, the species diversity of *Hypanus*
844 is far from taxonomic clarity, primarily due to unresolved species complexes and hidden
845 lineages, warranting additional revisions (Petean et al., 2024).

846 The findings of the present research resolve a taxonomic debate spanning nearly one and a
847 half century, originating with contemporaneous descriptions published by Jordan and Gilbert
848 (1880) and Garman (1880). By providing robust molecular and morphological evidence, this
849 study resurrects the Peruvian diamond stingray, *H. brevis* (ESP), from synonymy with *H.*
850 *dipterurus* (ENP). The resurrection of *H. brevis* as a distinct evolutionary unit from the ESP
851 was supported by the results of different molecular analyses conducted herein. The Bayesian
852 phylogenetic analysis recovered all specimens of *H. brevis* in a distinct monophyletic clade.
853 A mean distance of 4 % between the COI gene from *H. dipterurus* and *H. brevis* reinforce its

854 validation as a different species. The species status of both Pacific diamond stingrays was
855 further supported by AMOVA results. The high and significant Φ_{ST} values confirm that the
856 vast majority of genetic variation is partitioned between groups (ENP vs ESP), indicating
857 complete genetic isolation and lack of gene flow between them. Moreover, results of the
858 haplotype network analyses revealed a complete lineage sorting, with no haplotypes shared
859 between these two sister species.

860 Morphologically, *H. brevis* and *H. dipterurus* appear difficult to distinguish. Both species
861 share a generally similar disc shape, proportional measurements, dentition patterns, and
862 external coloration, resulting in considerable overlap in the characters traditionally used for
863 identification. Subtle differences have been suggested in previous studies; however, these
864 traits often show intraspecific variation and may be influenced by ontogeny or preservation
865 condition, reducing their diagnostic reliability. Consequently, the identification of these
866 species based solely on external morphology remains challenging and may lead to
867 misidentifications in the absence of comprehensive comparative material or additional lines
868 of evidence.

869 Garman (1880, 1883) and Lamilla et al. (1995) reported the presence of five oral papillae in
870 *H. brevis*. The present study likewise confirms five papillae on the floor of the mouth,
871 arranged in a transverse row, consisting of three well-developed medial papillae and one-
872 minute lateral papilla on each side, widely separated from the medial group. The small size
873 and inconspicuous nature of the lateral papillae may hinder their proper recognition.
874 Therefore, although the number of papillae appears consistent, careful examination is
875 required when assessing this character.

876 Dermal ornamentation in *H. brevis* has been recognized since the earliest descriptions as a
877 highly variable character, potentially associated with body size and age. Garman (1880,
878 1883), based on a large female, described the presence of three large, erect, broad-based

denticles located anterior to the caudal spine, as well as a rough tail bearing smaller tubercles. A similar pattern was observed in the present study on a large incomplete specimen of *H. brevis* (SV-0063), approximately 900 mm DW, whose tail exhibited more than 14 well-developed denticles (Figure 5h). Garman (1880, 1883) also noted short rows of one to four tubercles on the shoulder region, suggesting that their number likely increases with age, following a pattern comparable to that observed in closely related Atlantic species.

With respect to coloration, early descriptions already noted differences among *Hypanus* specimens along a latitudinal gradient. Jordan and Gilbert (1880) described specimens as light brown, slightly marbled with darker pigmentation, lacking distinct spots, and with a blackish tail. Subsequently, Beebe and Tee-Van (1941) observed that specimens from ENP exhibit a darker overall coloration, ranging from dark brown to nearly black. In contrast, specimens from the ESP display brown to olive, or slightly reddish tones. Nevertheless, these differences in pigmentation should be interpreted with caution, given the uncertainty surrounding the identity of the northern specimens. Broader comparative studies will be necessary to assess the taxonomic consistency of this trait and to rule out the influence of environmental or ontogenetic factors.

Regarding body size, specimen SV-0063 represents the largest documented record of *H. brevis* directly observed by the authors, reaching approximately 900 mm disc width (DW) (Figure 5h). Chirichigno and Cornejo (2001) reported maximum total lengths of up to 1.8 m TL. Although these larger sizes were not verified through examined material, they suggest that *H. brevis* may attain greater dimensions than currently represented in scientific collections.

The scarcity of large specimens in reference collections likely reflects logistical difficulties in capturing, handling, and preserving large rays rather than true rarity in nature. As a result, *H. brevis* remains poorly represented in museum collections and historically understudied.

Similar limitations have been reported for other Eastern Pacific chondrichthyans, where insufficient material constrains robust taxonomic and biological assessments (Becerril-García et al., 2022).

It has been proposed that the population history of the Pacific *Hypanus* lineages started during the Pliocene, with the formation of the Isthmus of Panama (Rosenberger, 2001). This major geological event occurred about three to four Ma (Thacker, 2017) and led to the allopatric speciation of three Pacific *Hypanus* lineages: *H. dipterurus*, *H. longus*, and *H. rubioi*, which branched off from their Atlantic transisthmian geminates: *H. say*, *H. americanus*, and *H. guttatus*, respectively (Mejía-Falla et al., 2025; Petean et al., 2024; Rosenberger, 2001). To get further insights into their evolutionary history, we employed the combined information from the COI and 16S rRNA genes to estimate their divergence times. Regrettably, the lack of 16S rRNA sequences in public databases for the recently discovered *H. rubioi* prevented us from dating its transisthmian divergence.

Our calibrated phylogenetic results dated the divergence time between *H. say* (Western Atlantic) and *H. dipterurus* (ENP) at approximately 3.42 Ma, while the subsequent split between *H. dipterurus* and *H. brevis* (ESP) was estimated at 3.09 Ma. These findings suggest that the monophyletic amphi-American lineage formed by these three *Hypanus* species emerged by an initial transisthmian vicariance (Jordan, 1908) followed by a secondary antitropical intra-Pacific radiation (Thacker, 2017). This two-step speciation model can be attributed to geological and oceanographic shifts that occurred during the gradual shoaling of the Central American Seaway (CAS), which lasted for approximately 12 million years (Lessios, 2008). These environmental drivers include intensified Pacific upwellings, cooler nutrient-rich deep waters, and salinity divergence (Carrillo-Briceño et al., 2018; O'Dea et al., 2016). During the Pliocene and Pleistocene, the Eastern Tropical Pacific was marked by dramatic changes in marine systems resulting in cold water upwelling zones (Ludt, 2021).

These lowered temperature zones during glacial periods potentially served as corridors enabling marine taxa to cross the Equator (Burridge, 2002; Ludt, 2021). After the glacial dispersal, warm tropical interglacial waters acted as a thermal barrier, pushing the ancestral Pacific populations toward the poles and leading to allopatric speciation (Lindberg, 1991).

The proposed "tropical gap" between *H. brevis* and *H. dipterurus* is currently based on a lack of confirmed occurrences in Central America. Our study analyzed genetically verified samples from the core populations of both species: *H. brevis* from the ESP (Peru) and *H. dipterurus* from the ENP (Mexico and southern USA). These locations represent typical temperate to subtropical waters, as defined by established marine ecoregions (Spalding et al., 2007). Although previous studies have reported low catch frequencies of *H. dipterurus* in Central America (e.g., Panama, Morales-Saldaña et al., 2025), these records may represent misidentifications. It is also likely that infrequent sightings of *H. dipterurus* in central American waters are merely transient range shifts triggered by climatic phenomena (Cerutti-Pereyra et al., 2024). In this light, further research is needed to confirm the actual geographic distribution boundaries of these stingrays.

The mean genetic distance of 4 % (see Table S1) observed between the COI gene of *H. dipterurus* and *H. brevis* represents a substitution rate of 1.22 % per million years. This rate is relatively high for elasmobranchs, which are known for their low mitochondrial mutation rates, estimated at a range of 0.2 to 0.3 % per million years (Martin et al., 1992). This can be a result of the rapid divergence between *H. dipterurus* and *H. brevis* following the closure of the CAS. These geminate species were forced to adapt to major shifting environments, triggering fast microevolutionary changes to maintain fitness in their new habitats (Knowlton & Weigt, 1998). Another explanation could be associated with the small effective population size that occurs when species experience a founder effect. Genetic drift can be more powerful

953 in small populations, leading to the fast fixation of new mutations (Slatkin & Excoffier,
954 2012).
955 A founder event could be also a possible speciation pathway in *H. brevis*. This event would
956 also explain the low intraspecific diversity in *H. brevis*, where a single, fixed haplotype was
957 detected in the COI gene. However, the divergence span of 3.09 Ma, suggested by our
958 molecular dating analysis, is more than enough for new mutations to accumulate and
959 establish different haplotypes (Dos Reis et al., 2015; Martin et al., 1992). The fixation of a
960 single COI haplotype across a wide latitudinal gradient (~3°S to 14°S), from the tropical
961 waters of Tumbes to the temperate-cold waters of Pisco, suggests high connectivity among
962 the Peruvian populations of *H. brevis*. High levels of gene flow among these populations are
963 likely facilitated by the northward movement of the Humboldt Current System (HCS) (Thiel
964 et al., 2007).
965 The low genetic variation observed among the Peruvian samples of *H. brevis* may be also the
966 result of genetic erosion driven by repetitive, high-intensity El Niño-Southern Oscillation
967 (ENSO) events that have occurred since the Late Pliocene (Oldeman et al., 2021). This
968 timeline coincides with the divergence age of *H. brevis* of approximately 3.09 Ma (Figure 4).
969 During extreme ENSO events, collapse of primary productivity in the HCS leads to mass
970 mortalities, which may have caused severe population bottleneck events in the Peruvian
971 diamond stingray, purging ancestral genetic variation (Arntz et al., 1991; Parouffe et al.,
972 2025). Alongside ENSO events, another possible driver of genetic erosion in Peruvian
973 populations of *H. brevis* is the highly selective fishing pressure that has targeted this
974 particular species for several decades. Myliobatiform rays, including *H. dipterurus*, are
975 known for their marked sexual size dimorphism, with females reaching larger sizes than
976 males (Smith, 2005). Peruvian artisanal fisheries frequently use gillnets selectively targeting

large individuals, which can lead to a loss of maternally-transmitted mitochondrial diversity and a reduced capacity to recover from depletion (Sadler et al., 2023).

The reduced genetic diversity of *H. brevis* is of particular conservation concern given that low genetic variation is often associated with a reduced adaptive potential to climatic changes (Reed & Frankman, 2003). While our genetic results indicate that *H. dipterurus* from the ENP showed classic signs of population expansion, *H. brevis* from the ESP, contrastingly, may have experienced a recent population bottleneck. This warrants immediate research on the ESP populations of the recently resurrected Peruvian diamond stingray lineage. These studies should conduct population genetic structure analyses and the estimation of effective population size using additional nuclear markers in more intensive geographic sampling. The results from these studies will determine whether the observed low mitochondrial variation in *H. brevis* reflects a critical population bottleneck or widespread connectivity within the Peruvian populations. Ultimately, these data will clarify the population's adaptive potential and enable the identification of management units needed for robust conservation strategies.

Conservation and management considerations

The taxonomic separation of *H. brevis* from *H. dipterurus* indicates that both species possess a more restricted distribution than previously understood when they were considered as a single species. Based on the available information, Peru serves as a significant hub for the fishing of *H. brevis* by small-scale operators, with certain reports indicating the presence of this species in northern Chile (Almendras et al., 2025; Bustamante et al., 2023) and Ecuador, including the Galápagos Islands (Alcivar Holguin & Pilligua Holguin, 2025; Bermello Vera, 2024; Grove et al., 2022; Victor et al., 2022). Moreover, further research is required to validate the distribution range and population structure, and to ascertain the exploitation status of the stock(s). *H. dipterurus* is a species that exhibits localized depletion due to its

intrinsic life-history traits and excessive fishing pressure (Smith et al., 2008). Given their close relatedness, the latter underscores the need to protect the two main fishing spots in Peru (see Figure 8), in a way to prevent future collapses of *H. brevis*, which exhibits remarkable mitochondrial homogeneity (see a discussion of area-based management mechanisms in Campos-León et al., 2025).

Considering the relative importance of the Peruvian fishery as the sole focus of regular fishing efforts throughout the years, it is a positive signal the fact that Peruvian landings have not experienced a sharp decline over the past three decades (Figure 7). Nonetheless, this should not be interpreted in isolation as an indicator of sustainable fishing practices. While catches may have remained relatively stable and provided a relatively consistent supply to markets over time, the unit of fishing effort may have increased, and/or the average size of caught individuals may have decreased. IMARPE maintains a comprehensive monitoring program for artisanal fisheries that likely contains relevant data that could thereby facilitate answering some of the relevant research questions to inform specific management provisions. Therefore, it is advisable to disclose existing biological and fisheries data and to develop plans for the collection of supplementary data (Campos-León et al., 2025; González-Pestana et al., 2022). Revision of the available datasets may lead to an update of the life-history traits, as until now most have been estimated solely through sampling *H. dipterurus* individuals within the ENP (Mariano-Meléndez, 1997; Restrepo-Gómez et al., 2020; Smith, 2005; Smith et al., 2008), while fewer studies have been conducted on the ESP *H. brevis*. With some exceptions, the life-history parameters of *H. brevis* remain largely undocumented (Garcia-Yarihuamán & Mantarí-Gavilano, 2021; González-Pestana et al., 2022; Sánchez Rea, 2020; Silva-Garay et al., 2018).

Finally, *H. dipterurus* is classified as a vulnerable species in its most recent assessment by the IUCN Red List of Threatened Species, considering that "[i]n Peru, directed gillnet fisheries

landings for this species have seen a decline of 50 % in annual landed biomass between 1997 and 2015 [...]" (Pollom et al., 2020). Our results, covering a longer period than the IUCN evaluation, do not show a declining landing trend. However, this should not be construed as an indicator of sustainable management, given that the fishery is undermanaged. Therefore, the absence of a clear definition of the exploitation status should not justify failure to implement management measures; instead, a more precautionary approach must be adopted, acknowledging the significant uncertainty and recognizing that the genetic diversity of the reclassified *H. brevis* is impoverished, serving as a potential proxy for population health that indicates conservation concerns. Consequently, it calls for further analyses to identify management strategies that prevent additional losses of genetic variation. Future IUCN evaluations should consider *H. brevis* as an independent species.

AUTHOR CONTRIBUTIONS

Alan Marín: conceived and designed the study, supervised the project, designed the molecular experiments, analyzed the data, conducted the population genetics/phylogenetic/evolutionary analyses, developed figures, wrote the first draft of the manuscript.

Fabiola Zavalaga: conceived and designed the study, conducted field work, conducted and led the morphometric analysis, analyzed the data, developed figures, wrote the original draft (morphometric sections).

Renato Gozzer-Wuest: conceived and designed the study, conducted the fisheries analysis, analyzed the data, developed figures, wrote the original draft (fisheries and conservation sections).

Luis E. Santos-Rojas: conducted field work, performed the molecular experiments, analyzed the data.

Lorenzo E. Reyes-Flores: conducted field work, performed the molecular experiments, analyzed the data.

Ruben Alfaro: conducted field work, performed the molecular experiments, analyzed the data.

Philippe Béarez: conceived and designed the study, conducted and led the morphometric analysis, analyzed the data, developed figures, reviewed and edited the manuscript, wrote the original draft (morphometric sections).

Eliana Zelada-Mázmela: conceived and designed the study, reviewed and edited the manuscript, provided laboratory facilities for molecular analysis, administered the project, responsible for funding acquisition.

All authors read, revised, and approved the final version of the manuscript.

ACKNOWLEDGEMENTS

The authors thank Luis Bancayán for providing photographic material and tissue samples of *H. longus* from Tumbes, Peru. We are grateful to R. Robertson and J. Quiñones for providing photographs of *H. americanus*, *H. brevis*, *H. sabinus*, and *H. say*. Special thanks are also extended to fisheries biologist Andrey Moreno for his assistance with the photographic documentation of *H. brevis* specimens deposited at IMARPE, as well as for his support in specimen handling.

CONFLICT OF INTEREST STATEMENT

The authors declare no conflict of interest.

DATA AVAILABILITY STATEMENT

All DNA sequences generated in the present study are available in the GenBank database under accession numbers from PZ027578 to PZ027634.

ORCID

Alan Marín https://orcid.org/0000-0001-7842-133X

Fabiola Zavalaga https://orcid.org/0000-0001-8680-4795

Renato Gozzer-Wuest https://orcid.org/0000-0002-1156-4552

Luis E. Santos-Rojas https://orcid.org/0000-0002-3756-6759

Lorenzo E. Reyes-Flores https://orcid.org/0000-0002-1993-8010

Ruben Alfaro https://orcid.org/0000-0001-8749-1647

Philippe Béarez https://orcid.org/0000-0003-0397-2393

Eliana Zelada-Mázmela https://orcid.org/0000-0002-5813-0954

REFERENCES

Alcivar Holguin, N. A., & Pilligua Holguin, I. A. (2025). Distribución temporal de batoideos capturados en Jaramijó-Manabí durante el 2024-2025. Universidad Laica Eloy Alfaro de Manabí, Manta Ecuador.

Almendras, D., Villafaña, J. A., Bustamante, C., Contreras, I., Campoy, A. N., Dufflocq, P., & Rivadeneira, M. M. (2025). New evidence confirms the presence of the diamond stingray *Hypanus dipterurus* (Jordan & Gilbert 1880) in Chile and extends its southern range. *Journal of Fish Biology*, *106*(4), 1245-1250.

Arntz, W. E., Tarazona, J., Gallardo, V. A., Flores, L. A., & Salzwedel, H. (1991). Benthos communities in oxygen deficient shelf and upper slope areas of the Peruvian and Chilean Pacific coast, and changes caused by El Niño. *Geological Society, London, Special Publications*, *58*(1), 131-154.

Aschliman, N. C., Nishida, M., Miya, M., Inoue, J. G., Rosana, K. M., & Naylor, G. J. (2012). Body plan convergence in the evolution of skates and rays (Chondrichthyes: Batoidea). *Molecular Phylogenetics and Evolution*, *63*(1), 28-42.

Ball, R. E., Serra-Pereira, B., Ellis, J., Genner, M. J., Iglésias, S., Johnson, A. F., ... & Griffiths, A. M. (2016). Resolving taxonomic uncertainty in vulnerable elasmobranchs: are the Madeira skate (*Raja maderensis*) and the thornback ray (*Raja clavata*) distinct species? *Conservation Genetics*, *17*(3), 565-576.

BCRP. (2025a). Data mensual, Serie de tiempo del tipo de cambio nominal. Retrieved from https://estadisticas.bcrp.gob.pe/estadisticas/series/mensuales/tipo-de-cambio-nominal

BCRP. (2025b). Data mensual, Serie de tiempo de inflación. Retrieved from https://estadisticas.bcrp.gob.pe/estadisticas/series/mensuales/inflacion.

Becerril-García, E. E., Arauz, R., Arellano-Martínez, M., Bonfil, R., Ayala-Bocos, A., Castillo-Géniz, J. L., Carrera-Fernández, M., Charvet, P., Chiaramonte, G., Cisneros-Montemayor, A. M., Concha, F., Espinoza, M., Ehemann, N. R., Estupiñán-Montaño, C., Fuentes, K., Galván-Magaña, F., Graham, R., Hacohen-Domené, A., Hazin, F., ...Godard-Codding, C. A. G. (2022). Research priorities for the conservation of chondrichthyans in Latin America. *Biological Conservation*, *269*, 109535. https://doi.org/10.1016/j.biocon.2022.109535

Beebe, W. & Tee-Van, J. (1941). Eastern Pacific expeditions of the New York Zoological Society. XXVIII. Fishes from the tropical eastern Pacific. Part 3. Rays, Mantas and Chimaeras. *Zoologica, Scientific Contributions of the New York Zoological Society*, *26* (3), 245–280.

Bermello Vera, K. S. (2024). Distribución y caracterización de la fauna acompañante en la pesca industrial de *Merluccius gay*i Merluza durante el año 2017–2022. La Libertad. UPSE, Matriz. Facultad de Ciencias del Mar. 98p.

Borsa, P., Arlyza, I. S., Chen, W. J., Durand, J. D., Meekan, M. G., & Shen, K. N. (2013). Resurrection of New Caledonian maskray *Neotrygon trigonoides* (Myliobatoidei: Dasyatidae) from synonymy with *N. kuhlii*, based on cytochrome-oxidase I gene sequences and spotting patterns. *Comptes Rendus. Biologies*, *336*(4), 221-232.

Burridge, C. P. (2002). Antitropicality of Pacific fishes: molecular insights. *Environmental Biology of Fishes*, *65*(2), 151-164.

Bustamante, C., Acuña, E., Tapia-Jopia, C., & Vargas-Caro, C. (2023). Actualización del Plan de Acción Nacional para la conservación y manejo de tiburones de Chile. Informe Final Proyecto del Fondo de Investigación Pesquera y de Acuicultura (FIPA N°2021-24). Universidad de Antofagasta.

Calle-Morán, M. D., & Béarez, P. (2020). Updated checklist of marine cartilaginous fishes from continental and insular Ecuador (Tropical Eastern Pacific Ocean). *Cybium*, *44*(3), 239-250.

Campos-León, S., Hernández-Muñoz, S., Huerta-Beltrán, B. L., Zavalaga, F., Cevallos-Garcias, A., & Ehemann, N. (2025). Peruvian Chondrichthyes biodiversity, marketing and conservation: a synthesis of current knowledge. *Journal of Fish Biology*. https://doi.org/10.1111/jfb.70227

Carrillo-Briceño, J. D., Carrillo, J. D., Aguilera, O. A., & Sanchez-Villagra, M. R. (2018). Shark and ray diversity in the Tropical America (Neotropics)—an examination of environmental and historical factors affecting diversity. *PeerJ*, *6*, e5313.

Cerutti-Pereyra, F., Drunkard, E., Espinoza, M., Finucci, B., Galván-Magaña, F., Hacohen-Domené, A., … & Chin, A. (2024). Vulnerability of Eastern Tropical Pacific chondrichthyan fish to climate change. *Global change and biology, 30*(7), e17373.

Chatzispyrou, A., & Koutsikopoulos, C. (2023). Tracing patterns and biodiversity aspects of the overlooked skates and rays (Subclass Elasmobranchii, Superorder Batoidea) in Greece. *Diversity*, *15*(1), 55.

Chen, M. Y., Liang, D., & Zhang, P. (2017). Phylogenomic resolution of the phylogeny of laurasiatherian mammals: exploring phylogenetic signals within coding and noncoding sequences. *Genome Biology and Evolution*, *9*(8), 1998-2012.

Chirichigno, N. (1974). *Clave para identificar los peces marinos del Perú*. Informe Instituto del Mar del Perú (IMARPE), Callao, Perú. 387 pp.

Chirichigno, N., & Vélez, J. (1998). *Claves para identificar los peces marinos del Perú*. 2ª edición. Instituto del Mar del Perú (IMARPE), Callao, Perú. 496 pp.

Chirichigno, N., & Cornejo, R.M. (2001). *Catálogo comentado de los peces marinos del Perú*. Instituto del Mar del Perú (IMARPE), Callao, Perú. 314 pp.

Cunha, Y. T. C., Leite, R. D., Pereira da Silva, L. G., Cruz, V. P., Nunes, J. L. S., Rotundo, M. M., ... & Sales, J. B. D. L. (2026). A comprehensive overview of evolutionary relationships and geographic distributions of cownose rays: more valid taxa needing protective measures. *Reviews in Fish Biology and Fisheries*, *36*(1), 37.

Dos Reis, M., Donoghue, P. C., & Yang, Z. (2016). Bayesian molecular clock dating of species divergences in the genomics era. *Nature Reviews Genetics*, *17*(2), 71-80.

Ebert, D.A. (2003). Sharks, Rays, and Chimaeras of California. University of California Press.

Ebert, D. A., Bigman, J. S., & Lawson, J. M. (2017). Chapter Two - Biodiversity, life history, and conservation of Northeastern Pacific Chondrichthyans. In S. E. Larson, & D. Lowry (eds), *Advances in marine biology* (Vol. 77, pp. 9-78). Academic Press.

Eschmeyer, W.N. (editor). 1998. Catalog of fishes. Spec. Publ. No. 1, Center for Biodiversity Research and Information. California Academy of Sciences, San Francisco. 483 pp.

Feitosa, L. M., Queiroz, A. P., Labonne, M., Dressler, V. L., & Lessa, R. P. (2021). Habitat use and nursery evaluation for the longnose stingray *Hypanus guttatus* (Bloch & Schneider, 1801) using vertebral microchemistry. *Journal of Fish Biology*, *99*(5), 1538-1549.

Fricke, R., Eschmeyer, W. N., & Fong, J. D. (2025). Eschmeyer's Catalog of Fishes: Genera/Species/References. (http://researcharchive.calacademy.org/research/ichthyology/catalog/fishcatmain.asp). Electronic version accessed 09 dec 2025.

Gabbanelli, V., de Astarloa, J. M. D., Gonzalez-Castro, M., Vazquez, D. M., & Mabragaña, E. (2018). Almost a century of oblivion: Integrative taxonomy allows the resurrection of the longnose skate *Zearaja brevicaudata* (Marini, 1933) (Rajiformes; Rajidae). *Comptes Rendus Biologies*, *341*(9-10), 454-470.

García-Yarihuamán, L. R., & Mantarí-Gavilano, P. J. (2021). Hábitos alimentarios de los batoideos de importancia comercial de Pisco-Ica, Mayo–Septiembre 2019. Undergraduate thesis. Universidad Nacional San Luis Gonzaga. Ica, Perú Available at: https://repositorio.unica.edu.pe/server/api/core/bitstreams/ee5ad01d-a16c-4f9f-9add-9be0280382e1/content.

Garman, S. (1880). New species of selachians in the museum collection. *Bulletin of the Museum of Comparative Zoology*, *6*(11), 167-172.

Garman, S. (1883). The American species of the genus *Dasibatis*. *In* D. S. Jordan & C. H. Gilbert (Eds.), Synopsis of the fishes of North America. *Bulletin of the United States National Museum*, *16*, 65-72.

Garman, S. (1913). The Plagiostomia. (Sharks, Skates, and Rays). *Memoirs of the Museum of Comparative Zoology*, *36*, 1-515.

Gayford, J. H., & Jambura, P. L. (2025). Drivers of diversification in sharks and rays (Chondrichthyes: Elasmobranchii). *Frontiers in ecology and evolution*, *12*, 1530326.

González-Pestana, A., Velez-Zuazo, X., Alfaro-Shigueto, J., & Mangel, J. C. (2022). Batoid fishery in Peru (1950-2015): Magnitude, management and data needs. *Revista de Biología Marina y Oceanografía*, *57* (Especial), 217-233.

Grove, J. S., Long, D. J., Robertson, D. R., & Victor, B. C. (2022). List of fishes of the Galapagos Archipelago, Ecuador. *Journal of the Ocean Science Foundation, 39*, 14-22.

Hosegood, J., Humble, E., Ogden, R., De Bruyn, M., Creer, S., Stevens, G. M., ... & Carvalho, G. (2020). Phylogenomics and species delimitation for effective conservation of manta and devil rays. *Molecular ecology*, *29*(24), 4783-4796.

Jordan, D. S. (1908). The law of geminate species. *The American naturalist, 42*(494), 73-80.

Knowlton, N., & Weigt, L. A. (1998). New dates and new rates for divergence across the Isthmus of Panama. *Proceedings of the Royal Society of London. Series B: Biological Sciences*, *265*(1412), 2257-2263.

IMARPE. (2025). INFOMAR: Proyecto Pesca Artesanal - Sistema de información de precios playa, mareas y oleajes. Retrieved from http://infomar.imarpe.gob.pe:8080/Acceso/Login?ReturnUrl=%2F

iNaturalist. (2026). iNaturalist Research-grade Observations. iNaturalist.org. Occurrence dataset https://doi.org/10.15468/ab3s5x accessed via GBIF.org on 2026-01-10. https://www.gbif.org/occurrence/1945421174

IUCN Standards and Petitions Committee. (2024). Guidelines for Using the IUCN Red List Categories and Criteria. Version 16. Prepared by the Standards and Petitions Committee. Downloadable from https://www.iucnredlist.org/documents/RedListGuidelines.pdf.

IUCN (2025). The IUCN Red List of Threatened Species. Version 2025-2. https://www.iucnredlist.org

Jordan, D. S., & Gilbert, C. H. (1880). Notes on a collection of fishes from San Diego, California. *Proceedings of the United States National Museum*, *3*, 23-24.

Kimura, M. (1980). A simple method for estimating evolutionary rates of base substitutions through comparative studies of nucleotide sequences. *Journal of molecular evolution*, *16*(2), 111-120.

Lamilla, J., Pequeño, G., & Kong, I. U. (1995). *Dasyatis brevis* (Garman, 1880) segunda especie de Dasyatidae registrada para Chile (Chondrichthyes, Myliobatiformes). *Estud. Oceanol*, *14*, 23-27.

Landemaine, O. (1991). Sélaciens nouveaux du Crétacé supérieur du Sud-Ouest de la France. Quelques apports à la systématique des élasmobranches. *Saga*, *1*, 1-45.

Last, P. R., Manjaji-Matsumoto, B. M., Naylor, G. J. P., & White, W. T. (2016a). Chapter 25 Stingrays: family Dasyatidae. In P. R. Last, W. T. White, M. R. de Carvalho, B. Séret, M. F. W. Stehmann, & G. J. P. Naylor (Eds.), *Rays of the World* (pp. 522-618). CSIRO Publishing, Clayton South, Australia.

Last, P. R., Naylor, G. J., & Manjaji-Matsumoto, B. M. (2016b). A revised classification of the family Dasyatidae (Chondrichthyes: Myliobatiformes) based on new morphological and molecular insights. *Zootaxa*, *4139*(3), 345-368.

Lessios, H. A. (2008). The great American schism: divergence of marine organisms after the rise of the Central American Isthmus. *Annual Review of Ecology, Evolution, and Systematics*, *39*(1), 63-91.

Lindberg, D. R. (1991). Marine biotic interchange between the northern and southern hemispheres. *Paleobiology*, *17*(3), 308-324.

Love, M. S., Mecklenburg C. W., Mecklenburg T. A., & Thorsteinson L. K. (2005). Resource inventory of marine and estuarine fishes of the west coast and Alaska: A checklist of North Pacific and Arctic Ocean species from Baja California to the Alaska-Yukon border. U. S. Department of the Interior, U. S. Geological Survey, Biological Resources Division, Seattle.

Ludt, W. B. (2021). Missing in the middle: a review of equatorially disjunct marine taxa. *Frontiers in Marine Science*, *8*, 660984.

Marín, A. (2025). The first complete mitogenome of the endangered spotted eagle ray, *Aetobatus ocellatus*, confirms species and family taxonomic status. *Genetica*, *153*(1), 34.

Marín, A., Serna, J., Robles, C., Ramírez, B., Reyes-Flores, L. E., Zelada-Mázmela, E., ... & Alfaro, R. (2018). A glimpse into the genetic diversity of the Peruvian seafood sector: Unveiling species substitution, mislabeling and trade of threatened species. *PLoS One*, *13*(11), e0206596.

Marín-Abanto, P. M. (2018). Fenix Package. Retrieved from https://github.com/PabloMBooster/fenix/blob/master/DESCRIPTION

Marín Soto, W., Medina Cruz, A., Castillo Mendoza, G., Estrella Arellano, C., Guardia Otárola, A., Guevara Carrasco, R., ... & Bertrand, A. (2017). Atlas de la pesca artesanal del mar del Perú. IMARPE-IRD, Lima, Perú, 183 pp.

Marshall, A. D., Compagno, L. J., & Bennett, M. B. (2009). Redescription of the genus *Manta* with resurrection of *Manta alfredi* (Krefft, 1868) (Chondrichthyes; Myliobatoidei; Mobulidae). *Zootaxa*, *2301*(1), 1-28.

Martin, A. P., Naylor, G. J., & Palumbi, S. R. (1992). Rates of mitochondrial DNA evolution in sharks are slow compared with mammals. *Nature*, *357*(6374), 153-155.

Martínez-Ortiz J. & García-Domínguez M. (2013). Guía de campo de condrictios del Ecuador: quimeras, tiburones y rayas / Chondrichthyes of Ecuador field guide. Chimaeras, sharks and rays. 246 p. Manta: Ministerio de Agricultura, Ganadería, Acuicultura y Pesca.

Mejía-Falla, P. A., & Navia, A. F., (2019). Checklist of marine elasmobranchs of Colombia. *Universitas Scientiarum*, *24*(1), 241-276.

Mejía-Falla, P. A., Navia, A. F., Cardeñosa, D., & Tavera, J. (2025). New Species of the Genus *Hypanus* (Dasyatidae) from the Eastern Tropical Pacific Ocean. *Ichthyology & Herpetology*, *113*(1), 44-60.

Miller, M. A., Pfeiffer, W., & Schwartz, T. (2010). Creating the CIPRES Science Gateway for inference of large phylogenetic trees. *2010 Gateway Computing Environments Workshop (GCE), New Orleans, USA* (pp. 1-8).

Miller, E. F., Dossett, W. H., & Rankin, J. L. (2014). Clarifying the northern extent of the diamond stingray (*Dasyatis dipterura*) in Southern California. Bulletin, Southern California Academy of Sciences, *113*(3), 232-235.

Morales-Saldaña, J. M., Guzmán, H. M., Vega, A. J., Robles, Y. A., Montes, L. A., & Kyne, P. M. (2025). A review of the status of sharks, rays and chimaeras of Panama to guide research and conservation. *Aquatic Conservation: Marine and Freshwater Ecosystems*, *35*(4), e70122.

Mundy, B. C. (2005). Checklist of the fishes of the Hawaiian Archipelago. *Bishop Museum Bulletins in Zoology*, *6*, 1-703.

Naylor, G. J. P., Caira, J. N., Jensen, K., Rosana, K. A. M., White, W. T., & Last, P. R. (2012). A DNA sequence–based approach to the identification of shark and ray species and its implications for global elasmobranch diversity and parasitology. *Bulletin of the American Museum of Natural History*, *367*, 1-262.

Nelson, J. S., Crossman, E. J., Espinosa-Pérez, H., Findley, L. T., Gilbert, C. R., Lea, R. N., & Williams, J. D. (2004). *Common and scientific names of fishes from the United States, Canada and Mexico.* American Fisheries Society. Special Publication 29, Bethesda, Maryland. 192 pp.

Nishida, K., & Nakaya, K. (1990). Taxonomy of the genus *Dasyatis* (Elasmobranchia, Dasyatidae) from the North Pacific. In: Pratt Jr., H. L., S. H. Gruber and T. Taniuchi (eds.): *Elasmobranchs as living resources: advances in the biology, ecology, systematics, and the status of the fisheries*. NOAA (National Oceanic and Atmospheric Administration) Tech. Rept. NMFS 90:327-346.

Nylander, J. A., Ronquist, F., Huelsenbeck, J. P., & Nieves-Aldrey, J. (2004). Bayesian phylogenetic analysis of combined data. *Systematic biology*, *53*(1), 47-67.

O'Dea, A., Lessios, H. A., Coates, A. G., Eytan, R. I., Restrepo-Moreno, S. A., Cione, A. L., ... & Jackson, J. B. (2016). Formation of the Isthmus of Panama. *Science advances*, *2*(8), e1600883.

Oldeman, A., Baatsen, M., von Der Heydt, A., Dijkstra, H., Tindall, J., Abe-Ouchi, A., …& Williams, C. (2021). Reduced El Niño variability in the mid-Pliocene according to the PlioMIP2 ensemble. *Climate of the Past, 17*(6), 2427-2450.

Palumbi, S. R., Martin, A. P., Romano, S., McMillan, W. O., Stice, L., Grabowski, G. (1991). The simple fool's guide to PCR. Department of Zoology-University of Hawaii, Special Publication, Honolulu.

Parouffe, A., Dewitte, B., Paulmier, A., & Garçon, V. (2025). ENSO modulates aerobic habitat across varying hypoxia tolerance levels in the Southeast Pacific throughout the twenty-first century. *Scientific Reports*, *15*(1), 20670.

Petean, F. F., Naylor, G. J., & Lima, S. M. (2020). Integrative taxonomy identifies a new stingray species of the genus *Hypanus* Rafinesque, 1818 (Dasyatidae, Myliobatiformes), from the Tropical Southwestern Atlantic. *Journal of Fish Biology*, *97*(4), 1120-1142.

Petean, F. F., Yang, L., Corrigan, S., Lima, S. M., & Naylor, G. J. (2024). How many lineages are there of the stingrays genus *Hypanus* (Myliobatiformes: Dasyatidae) and why does it matter? *Neotropical Ichthyology*, *22*, e230046.

Philippe, H., Brinkmann, H., Lavrov, D. V., Littlewood, D. T. J., Manuel, M., Wörheide, G., & Baurain, D. (2011). Resolving difficult phylogenetic questions: why more sequences are not enough. *PLoS biology*, *9*(3), e1000602.

Pollom, R., Bizzarro, J., Burgos-Vázquez, M.I., Cevallos, A., Velez-Zuazo, X., Avalos, C., Espinoza, M., González, A., Herman, K., Mejía-Falla, P.A., Navia, A.F., Pérez Jiménez, J.C., & Sosa-Nishizaki, O. (2020). *Hypanus dipterurus*. The IUCN Red List of Threatened Species 2020: e.T60152A80677563. https://dx.doi.org/10.2305/IUCN.UK.2020-3.RLTS.T60152A80677563.en. Accessed on 22 November 2025.

Puentes, V., Mejía-Falla, P. A., Ramirez, J. G., Manjarrés-Martínez, L. M., Rguez-Baron, J. M., Zapata, L. A., ... & Navia, A. F. (2022). Sharks and marine batoids management in Colombia: Policy instruments, management duty and implications for their populations and stakeholders. *Marine Policy*, *145*, 105264.

Rambaut, A., Drummond, A. J., Xie, D., Baele, G., & Suchard, M. A. (2018). Posterior summarization in Bayesian phylogenetics using Tracer 1.7. *Systematic biology*, *67*(5), 901-904.

Reed, D. H., & Frankham, R. (2003). Correlation between fitness and genetic diversity. *Conservation biology*, *17*(1), 230-237.

Restrepo-Gómez, D. C., Cruz-Escalona, V. H., Peterson, M. S., Mejía-Falla, P. A., & Navia, A. F. (2020). Effects of age, maturity stage, sex and seasonality on the feeding strategies of the diamond stingray (*Hypanus dipterurus*) in the southern Gulf of California. *Marine and Freshwater Research, 72*(4), 469-480.

Robertson, D. R., & Van Tassell, J. (2023). Shorefishes of the Greater Caribbean: online information system. Version 3.0 Smithsonian Tropical Research Institute, Balboa, Panamá.

Rosenberger, L. J. (2001). Phylogenetic relationships within the stingray genus *Dasyatis* (Chondrichthyes: Dasyatidae). *Ichthyology & Herpetology*, *2001*(3), 615-627.

Sabaj, M. H. (2020). Codes for natural history collections in ichthyology and herpetology. *Ichthyology & Herpetology*, *108*(3), 593-669.

Sadler, D. E., Watts, P. C., & Uusi-Heikkilä, S. (2023). The riddle of how fisheries influence genetic diversity. *Fishes*, *8*(10), 510.

Sales, J. B. L., de Oliveira, C. N., dos Santos, W. C. R., Rotundo, M. M., Ferreira, Y., Ready, J., ... & da Silva Rodrigues-Filho, L. F. (2019). Phylogeography of eagle rays of the genus *Aetobatus*: *Aetobatus narinari* is restricted to the continental western Atlantic Ocean. *Hydrobiologia*, *836*(1), 169-183.

Sánchez Rea, A. B. (2020). Caracterización morfológica de las estructuras dérmicas de rayas (Chondrichthyes: batoidea) desembarcadas en el litoral peruano. Undergraduated thesis. Universidad Científica del Sur. Lima, Peru Available at: https://repositorio.cientifica.edu.pe/handle/20.500.12805/1333.

Silva-Garay, L., Pacheco, A. S., & Vélez-Zuazo, X. (2018). First assessment of the diet composition and trophic level of an assemblage of poorly known chondrichthyans off the central coast of Peru. *Environmental Biology of Fishes*, *101*(10), 1525-1536.

Simental-Anguiano, M. D., Torres-Rojas, Y. E., Galván-Magaña, F., & Tripp-Quezada, A. (2022). Importance of Shellfish in the Diet of Two Ray Species (*Rhinoptera steindachneri* and *Hypanus dipterurus*) in the Upper Gulf of California. *Journal of Shellfish Research*, *41*(2), 291-299.

Siskey, M. R., Shipley, O. N., & Frisk, M. G. (2019). Skating on thin ice: Identifying the need for species-specific data and defined migration ecology of Rajidae spp. *Fish and Fisheries*, *20*(2), 286-302.

Slatkin, M., & Excoffier, L. (2012). Serial founder effects during range expansion: a spatial analog of genetic drift. *Genetics*, *191*(1), 171-181.

Smith, W. D. (2005). Life history aspects and population dynamics of a commercially exploited stingray, *Dasyatis dipterura* (Doctoral dissertation, San Francisco State University).

Smith, W. D., Cailliet, G. M., & Cortés, E. (2008). Demography and elasticity of the diamond stingray, *Dasyatis dipterura*: parameter uncertainty and resilience to fishing pressure. *Marine and Freshwater Research, 59*(7), 575-586.

Spalding, M. D., Fox, H. E., Allen, G. R., Davidson, N., Ferdaña, Z. A., Finlayson, M. A. X., ... & Robertson, J. (2007). Marine ecoregions of the world: a bioregionalization of coastal and shelf areas. *BioScience*, *57*(7), 573-583.

Spöri, Y., & Flot, J. F. (2020). HaplowebMaker and CoMa: two web tools to delimit species using haplowebs and conspecificity matrices. *Methods in Ecology and Evolution*, *11*(11), 1434-1438.

Thacker, C. E. (2017). Patterns of divergence in fish species separated by the Isthmus of Panama. *BMC Evolutionary Biology*, *17*(1), 111.

Thiel, M., Macaya, E., Acuña, E., Wolf, E. A., Bastias, H., Brokordt, K., …& Vega, A. (2007). The Humboldt Current System of northern and central Chile. *Oceanography and Marine Biology: An Annual Review*, *45*, 195-344.

Victor, B. C., Grove, J. S., Long, D. J., Robertson, D. R., Keith, I., Bensted-Smith, W., & Salinas-de-León, P. (2024). List of fishes of the Galapagos archipelago, Ecuador (version 2.0). *Journal of the Ocean Science Foundation*, *41*, 54-111.

Ward, R. D., Zemlak, T. S., Innes, B. H., Last, P. R., & Hebert, P. D. (2005). DNA barcoding Australia's fish species. *Philosophical transactions of the royal society B: biological sciences*, *360*(1462), 1847-1857.

White, W. T. Last, P. R., Naylor, G.J.P., Jensen, K., & Caira, J. (2010). Clarification of *Aetobatus ocellatus* (Kuhl, 1823) as a valid species, and a comparison with *Aetobatus narinari* (Euphrasen, 1790) (Rajiformes: Myliobatidae). *CSIRO Marine and Atmospheric Research Paper*, *32*, 141.

White, W. T., & Last, P. R. (2012). A review of the taxonomy of chondrichthyan fishes: a modern perspective. *Journal of Fish Biology*, *80*(5), 901-917.

White, W. T., O'Neill, H. L., & Naylor, G. J. (2022). Taxonomy and diversity of extant elasmobranchs. In W. T. White, H. L. O'Neill, & G. J. Naylor (eds), *Biology of sharks and their relatives* (pp. 31-57). CRC Press.

Xia, X. (2018). DAMBE7: New and improved tools for data analysis in molecular biology and evolution. *Molecular biology and evolution*, *35*(6), 1550-1552.

Yamaguchi, A., Furumitsu, K., & Wyffels, J. (2021). Reproductive biology and embryonic diapause as a survival strategy for the East Asian endemic eagle ray *Aetobatus narutobiei*. *Frontiers in Marine Sciences 8*:768701

Zuccarello, G. C., & Lokhorst, G. M. (2005). Molecular phylogeny of the genus *Tribonema* (Xanthophyceae) using rbc L gene sequence data: monophyly of morphologically simple algal species. *Phycologia*, *44*(4), 384-392.

Supplementary material

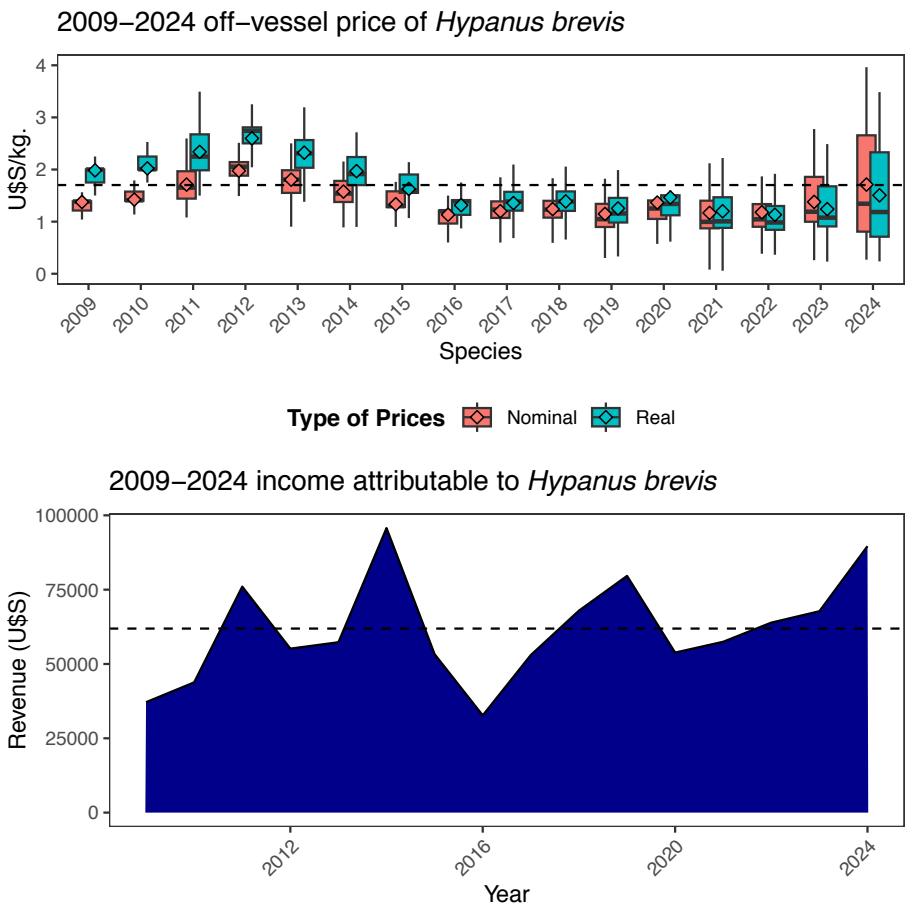

FIGURE S1 Box-plot with the off-vessel 2009-2024 prices of *Hypanus brevis* (top-panel) and the landing income attributable to this species during the same period (bottom-panel). The horizontal dashed line represents the average 2015-2024 annual income.

1557 **TABLE S1** Group interspecific mean distances of a partial COI fragment of five *Hypanus* species from the
1558 Pacific (*H. brevis*, *H. dipterurus*, and *H. longus*) and Atlantic Oceans (*H. americanus* and *H. say*). Analyses
1559 were conducted using the Kimura 2-parameter model. Interspecific mean distances are shown below the
1560 diagonal, while standard error estimates are shown above the diagonal. The last column shows the mean
1561 intraspecific distances and their standard error estimates between parenthesis. ESP: Eastern South Pacific; ENP:
1562 Eastern North Pacific; WA: Western Atlantic; WNA: Western North Atlantic.
1563

Species (n: sample size)	***H. brevis* (ESP)**	***H. dipterurus* (ENP)**	***H. say* (WA)**	***H. longus* (ESP)**	***H. americanus* (WNA)**	**Mean intraspecific distance (SD)**
***H. brevis* (n = 27)**	-	±0.0090	±0.0118	±0.0178	±0.0153	0.0000
***H. dipterurus* (n = 8)**	0.0397	-	±0.0110	±0.0145	±0.0151	0.0035 (±0.0015)
***H. say* (n = 4)**	0.0650	0.0578	-	±0.0145	±0.0149	0.0013 (±0.0012)
***H. longus* (n = 7)**	0.0984	0.1063	0.1063	-	±0.0066	0.0033 (±0.0019)
***H. americanus* (n = 4)**	0.1014	0.1046	0.1073	0.0249	-	0.0026 (±0.0018)

1564